ELECTROCHEMISTRY RESEARCH LABORATORY

DEPARTMENT OF CHEMISTRY
JOHN SCHOFF MILLIS SCIENCE CENTER
CASE WESTERN RESERVE UNIVERSITY
CLEVELAND, OHIO

TECHNICAL REPORT NO. 22

KINETIC STUDIES OF THE OXYGEN-PEROXIDE COUPLE ON PYROLYTIC GRAPHITE

by

Ikram Morcos and Ernest Yeager

1 December 1968

Office of Naval Research
Contract N00014-67-C-0389
Project NR 359-277

OFFICE OF NAVAL RESEARCH

Contract N00014-67-C-0389

Project NR 359-277

TECHNICAL REPORT NO. 22

KINETIC STUDIES OF THE OXYGEN-PEROXIDE COUPLE ON PYROLYTIC GRAPHITE

by

Ikram Morcos and Ernest Yeager

Department of Chemistry

CASE WESTERN RESERVE UNIVERSITY

Cleveland, Ohio 44106

1 December 1968

unclassified
Security Classification

DOCUMENT CONTROL DATA - R & D

(Security classification of title, body of abstract and indexing annotation must be entered when the overall report is classified)

1. ORIGINATING ACTIVITY (Corporate Author)

Case Western Reserve University
Cleveland, Ohio 44106, USA

2a. REPORT SECURITY CLASSIFICATION
Unclassified

2b. GROUP
---

3. REPORT TITLE

KINETIC STUDIES OF THE OXYGEN-PEROXIDE COUPLE ON PYROLYTIC GRAPHITE

4. DESCRIPTIVE NOTES (Type of report and inclusive dates)

Technical Report No. 22

5. AUTHORS (LAST NAME, FIRST NAME, INITIAL)

Marcos, Ikram, and Yeager, Ernest

6. REPORT DATE	7a. TOTAL NO. OF PAGES	7b. NO. OF REFS
1 December 1968	45	19

8a. CONTRACT OR GRANT NO.	9a. ORIGINATOR'S REPORT NUMBER(S)
N00014-67-C-0389	Technical Report No. 22
b. PROJECT NO. NR 359-277	9b. OTHER REPORT NO(S) (Any other numbers that may be assigned this report)
	---

10. DISTRIBUTION STATEMENT

This document has been approved for public release and sale; its distribution is unlimited

11. SUPPLEMENTARY NOTES	12. SPONSORING MILITARY ACTIVITY
---	Office of Naval Research Washington, D. C. 20360 Code 472, Chemistry Program

13. ABSTRACT

The cathodic and anodic properties of the oxygen-peroxide couple have been studied on ordinary pyrolytic graphite, high pressure annealed pyrolytic graphite and single crystal graphite in alkaline solutions using the rotating disc technique. Both the reduction of O_2 and oxidation of peroxide are inhibited on the cleavage surface of the oriented graphite relative to the edge surface. This difference in behavior is attributed to the lack of suitable adsorption sites on the cleavage surface for the reacting species and/or intermediates. The current-potential data, reaction orders, and stoichiometric number support the following mechanism: $O_2 \rightarrow O_2(ads)$; $O_2(ads) + HOH + e \rightarrow HO_2(ads) + OH^-$; $2\ HO_2(ads) + OH^- \rightarrow HO_2^- + O_2 + HOH$, with the first and second steps rate controlling for the cathodic reduction.

Unclassified
Security Classification

DOCUMENT CONTROL DATA - R & D (continued)

14. KEY WORDS

Oxygen electrode

Oxygen-peroxide couple

Rotating disc electrode

Graphite electrodes

Electrochemical kinetics

Electrode processes

TABLE OF CONTENTS

LIST OF FIGURES

LIST OF FIGURES (Continued)

LIST OF TABLES

KINETIC STUDIES OF THE OXYGEN-PEROXIDE COUPLE ON PYROLYTIC GRAPHITE

by

Ikram Morcos[a] and Ernest Yeager
Department of Chemistry
Case Western Reserve University
Cleveland, Ohio

INTRODUCTION

Oxygen is quantitatively reduced to peroxide on carbon and graphite in alkaline solutions[1-3]. The further reduction to the hydroxide usually does not occur at an appreciable rate on such surfaces in the absence of added catalysts. Isotopic studies[2] with O^{18} have indicated that the reduction of O_2 to HO_2^- as well as the reverse anodic process do not involve the actual rupture of the O-O bond but rather just the modification of the bond type.

In earlier work in the authors' laboratory[3] the current-potential curves for this couple were determined on various carbons and graphites using the rotating disc technique to control transport of reactants and products through the solution phase. The cathodic overpotential was found to be a linear function of log $[i/(i_d-i)]$ with a slope of approximately -0.12 V/decade, where i and i_d are the current density and diffusion limiting value for such, respectively. The apparent exchange current density was found to show surprisingly little variation among the several types of carbon and graphite examined.

On the basis of the observed cathodic Tafel slope (-0.12 V/decade) and the first order dependence of the kinetics of the reduction on dissolved O_2

---

[a] Now at McGill University, Montreal, Canada.

concentration, the rate-determining step for the O_2 reduction was suggested to be the one-electron transfer process

$$O_2 + e^- \rightleftharpoons O_2^-(ad) \qquad (1)$$

with a value for the transfer coefficient of 1/2. It is interesting to note that the superoxide anion O_2^- has been shown to be a rather stable intermediate in O_2 reduction in aprotic solvents in the work of Maricle and Hodgson[4].

An important question which was not resolved in the earlier work was the role of the carbon surface and in particular whether the reduction proceeds more readily on the cleavage surface which exposes the aromatic π-orbital electrons or the edge (parallel to the C axis) which should be covered with various C-H-O chemical groups. The availability of highly oriented pyrolytic graphites as well as single crystal graphite permits this question to be resolved. The examination of the kinetics of the O_2-peroxide couple on such surfaces has been the objective of the present work.

EXPERIMENTAL PROCEDURE

Current-voltage curves have been obtained by slow linear sweep voltammetry with a Wenking potentiostat and a motor-driven potentiometer as a source of scanning voltage. An x-y plotter (Houston Instruments, Model HR-96) was used to record the current as a function of potential. All results reported in this paper are for a scanning rate of 1 V/min. Slower scanning rates also have been examined but no significant differences were found.

The measurements have been carried out on various pyrolytic graphites[b] as well as single crystal graphite[b]. The latter was naturally occurring and was leached out of a block of marble with hydrofluoric acid, followed by purification with high temperature treatment with chlorine. All of the pyrolytic

---

[b] These materials were supplied by the Union Carbide Research Center, Parma, Ohio.

graphites were produced by decomposing hydrocarbons at elevated temperatures (≈1800°C). Of special interest are the measurements on those pyrolytic graphites which were subjected to high pressure-high temperature annealing at 3000°C. These materials are similar to those described by Ubbelohde et al.[5] and have a well developed laminar structure and the appearance of black mica. Both the cleavage and edge surfaces have been examined electrochemically.

The rotating disc technique[6] has been used to control mass transport in all of the measurements reported herein. Because of the fragile nature of the electrodes and the difficulty of preparing electrodes in cylindrical shapes, the electrodes were not force fitted into Teflon cylinders as in the earlier work[3] at Case Western Reserve but rather compression moulded into Kel-F[c] holders. The graphite electrode was placed at the bottom of a chromium plated stainless steel cylinder which then was filled with granules of Kel-F. The cylinder was next heated to 300°C for 30 min. with a piston pressure of 40 atm and allowed to cool down to room temperature at this pressure. The Kel-F cylinder with the graphite electrode at the bottom was machined to the required dimensions and compression fitted into a Teflon-coated steel shaft.

All of the ordinary pyrolytic graphite electrodes and the high pressure annealed graphite electrodes with the cleavage plane exposed to the solution had disc-shaped surfaces with areas of ≈0.2 cm^2. In prior work[3] the dependence of the limiting current on the rotation rate has been examined with this type of rotating disc electrode for the tri-iodide ion reduction. The results were virtually identical (within 2% when normalized for radius) to those reported by Nelson and Riddiford[7] for rotation rates from 100 to 1800 rpm.

For the edge orientation of the high pressure annealed pyrolytic graphite and the single crystal graphite, non-circular surfaces approximating a square

---

[c] This polymer (polychlorotrifluoroethylene) was supplied in the form of moulding powderby the Minnesota Mining and Manufacturing Co.

were exposed to the solution because of difficulties encountered in attempts to machine di . In other studies[8] in the authors' laboratory, a comparison has been made of the oxidation of ferrocyanide on square (0.201 cm^2) and circular (0.185 cm^2) nickel electrodes mounted in a Kel-F cylinder of the same diameter (1.1 cm) as used in the present study. The limiting current density was found to be the same within 3% for the two electrodes at all of the rotation rates examined (900-6400 rpm). The shapes of the current-voltage curves also were nearly the same in a 0.005 M $K_3Fe(CN)_6$, 0.005 M $K_4Fe(CN)_6$, 0.5 M K_2SO_4 solution. Consequently it does not appear that any substantial error was introduced in the present studies by the use of square graphite electrodes for part of the measurements.

For the cleavage surface of both the high pressure annealed pyrolytic graphite and the single crystal graphite, a fresh surface was exposed by placing a piece of plastic adhesive tape in contact with the graphite surface and then pealing off a thin layer with the tape. The surface so exposed had the appearance of a black mirror. The adhesive covered surface of the plastic tape was not touched to the Kel-F mounting. With the edge orientation of the high pressure annealed pyrolytic graphite and the ordinary pyrolytic graphite, a fresh surface was exposed by removing a thin graphite layer with a sharp stainless steel cutting edge. To maintain co-planarity of the electrode surface with that of the Kel-F mounting, the graphite electrode was pushed forward slightly in the Kel-F mounting after the surface was pealed or cut each time. This was not possible with the single crystal graphite because of its irregular shape.

The only treatment given to the pyrolytic and single crystal graphite electrodes after machining or cleaving was a thorough rinsing with 1 M KOH solution.

The cell (Fig. 1) was constructed entirely of Teflon except for the graphite electrode mounting and the Hg/HgO,1 M KOH reference electrode

compartment which was made of Pyrex glass. The reference electrode compartment was well isolated from the main cell compartment by a Teflon solution bridge and a Teflon intermediate compartment. A Luggin capillary made of Teflon was press fitted into the end of the solution bridge inside the cell. The tip of the Luggin capillary extended to ≈3 mm below the surface of the graphite working electrode (see Fig. 1). The counter electrode consisted of a bright platinum (99.99% pure) sheet, 3.0 x 4.0 x 0.007 cm in dimension. The platinum sheet was spot welded to platinum wire of equal purity and was vertically mounted near the wall of the cell by means of a Teflon support rod extending down from the Teflon cover of the cell. The cell had a volume of 250 cm^3 and was usually 3/4 filled.

Except where otherwise noted, the measurements were carried out in 1 M KOH solutions prepared from Baker reagent grade KOH pellets (0.2% carbonate) and triply distilled water. No attempt was made to remove the carbonate initially present in the KOH. For some of the measurements, a known volume of standardized 1-2 M H_2O_2 solution was also added to the KOH solution. The peroxide solution was prepared from unstabilized 90% hydrogen peroxide (Buffalo Electrochemical Co.) and triply distilled water. After the completion of a set of measurements a sample of solution was withdrawn from the cell and the peroxide concentration determined by titration with potassium permanganate solution. The hydroxide ion concentration was also determined by titration with a standardized acid solution.

The commercial oxygen gas (Ohio Chemical Co.) used in this study was purified by means of a gas train which included Hopcalite (Mine Safety Appliance Co.) to convert CO to CO_2, and high area rutile (TiO_2) in a dry ice-acetone trap to adsorb any organic residuals. The helium gas (Ohio Chemical Co.) used to agitation the solution during pre-electrolysis was purified by passing it through a gas train which included heated copper turnings to remove O_2 and silica gel in a liquid nitrogen trap to remove other impurities.

Before each series of measurements the solution was pre-electrolyzed within the Teflon cell between two ancillary bright platinum electrodes (4 cm^2 each) at a cell voltage of 1.4 V for at least 24 hrs with agitation provided by bubbling purified helium thorugh the solution. The pre-electrolysis electrodes were removed from the solution after the completion of the pre-electrolysis.

The use of platinum for a counter electrode and pre-electrolysis electrodes leads to contamination of the solution with platinum but it is very difficult to find other electrode materials which do not present similar difficulties. In other studies[9] of oxygen reduction kinetics on gold in alkaline solutions, the trace platinum has been found to cause irreproducibility probably because of changes in the extent of coverage of the gold with platinum and the form of the platinum on the gold surface. In the present study the cathodic measurements were quite reproducible. Furthermore the reduction of O_2 on platinum usually yields close to 4 electrons per O_2 in contrast to the present measurements on graphite where only 2 electrons per O_2 were obtained. It is interesting to note that the cathodic measurements made with and without prior pre-electrolysis gave essentially the same results. The level of platinum contamination should be increased with such pre-electrolysis and thus the lack of any significant difference provides further evidence that platinum contamination was not an important factor.

EXPERIMENTAL RESULTS

In Figs. 2 and 3 is shown the dependence of the cathodic current on potential for various rotation rates on the edge surface of high pressure annealed pyrolytic graphite and the cleavage surface of ordinary pyrolytic graphite in the absence of initially added peroxide. The directions of the voltage sweeps are indicated by the arrows. The hysteresis shown in Fig. 2 is typical for voltage sweeps starting from potentials of 0 and

extending to ~-0.6 V re. Hg/HgO, 1 M KOH. Unless otherwise indicated the data obtained with increasingly cathodic potentials have been used in subsequent graphs. The dependence of the cathodic current on the square root of the rotation rate is shown in Figs. 4 and 5 for these same graphite surfaces for a fixed potential corresponding to the maxima in the current in Figs. 2 and 3 (-0.43 V re. Hg/HgO, 1 M KOH). The curvature indicates combined diffusion and kinetic control.

If first order kinetics with respect to dissolved molecular O_2 are involved, the observed currents are related to the rotation rate ω in radians/sec by the equation

$$\frac{1}{I_L} = \frac{1}{I_k} + \frac{1}{AB\sqrt{\omega}} = \frac{1}{I_k} + \frac{1}{B'\sqrt{f}} \qquad (1)$$

where the diffusion limiting current $I_d = AB\sqrt{\omega}$, i_k is the current corresponding to pure kinetic control, A is the disc electrode area, f is the rotation rate in rpm, and B is given by Newman[10] as

$$B = nF\,\nu^{1/2}\,C_o \cdot [0.621\,S^{-2/3}/(1 + 0.298\,S^{-1/3} + 0.145\,S^{-2/3})] \qquad (1a)$$

and

$$B' = AB\sqrt{2\pi/60} \qquad (1b)$$

where ν is the kinematic viscosity, D is the diffusion coefficient, F is the Faraday, n is the number of electrons per mole of O_2, C_o is the concentration of O_2 in moles/cm^3, and the Schmidt number is $S = \nu/D$. The plots in Figs. 6 and 7 indicate that the experimental data follow eq. (1) at least approximately for various fixed potentials including that corresponding to the maxima in Figs. 2 and 3. The slope varies somewhat at various potentials for the edge orientation of the high pressure annealed graphite perhaps because of the use of a rectangular rather than circular electrode.

The straight lines in Figs. 4 and 5 represent the diffusion limiting currents (I_d) determined from the plots in Figs. 6 and 7 using eq. (1).

The calculation of the values for B' corresponding to the slopes of these straight lines in Figs. 4 and 5 from eqs. (1a,b) is complicated by some uncertainty as to the diffusion coefficient for O_2 in 1 M KOH. The measurements of Davis et al.[11] using the rotating disc technique and also a stagnant tube technique indicate a value of $D = 1.44 \times 10^{-5}$ cm^2/sec in 1 M KOH at 25°C while those of Gubbins and Walker[12] using the polarographic technique yield a value of $D = 1.65 \times 10^{-5}$ cm^2/sec. This difference is somewhat greater than would be anticipated on the basis of the precision of the measurements. Gubbins and Walker estimate their maximum error to be ± 6%. Davis et al.[11] assume a four-electron reduction of O_2 on both silver and platinum but such depends on the surface condition of the electrode and the purity of the electrolyte. No evidence is presented to substantiate that the reductions yielded exactly 4 electrons per O_2. This is not a problem with the polarographic technique where two distinct two-electron waves are observed. Gubbins and Walker used the first wave and the quite reliable modified Ilkovic equation[13]. Consequently the values for the diffusion coefficients obtained by Gubbins and Walker appear more reliable.

Values for B' for the disc and rectangular electrodes have been calculated by means of eqs. (1a,b) using the solubility data for O_2 of Davis et al.[1] interpolated to 22°C (S = 0.87 mM at a total pressure of 1 atm) and the diffusion coefficient data of Gubbins and Walker at 25°C ($D_{O_2} = 1.65 \times 10^{-5}$ cm^2/sec) corrected to 22°C ($D_{O_2} = 1.53 \times 10^{-5}$ cm^2/sec) using the mean temperature coefficient estimated from the data of Davis et al. ($\partial \ln D_{O_2}/\partial T = 2.4\%/°C$). The experimental and calculated values for B' are shown in Table I.

TABLE I. Comparison of experimental and calculated values for B'.

Pyrolytic graphite electrode	$-B' \times 10^2$ (mA/$\sqrt{\text{sec}}$) experimental[a]	calculated[b]
1. Disc electrode (A = 0.196 cm^2) (ordinary)	1.0_3	0.86
2. Rectangular electrode (A = 0.22 cm^2) (high pressure annealed)	1.1_1	0.97

[a] Determined from Figs. 6 and 7 using eq. (1).

[b] Based on two electrons per O_2.

The calculated values are approximately 15% lower than the experimental values based on a two-electron process. Such a deviation is relatively small but not negligible and may reflect some small deviation from two-electrons per O_2 molecule diffusing to the electrode either because of subsequent reduction or surface-catalyzed decomposition of some of the peroxide generated at the electrode or direct reduction of O_2 to water without peroxide in solution as an intermediate. To check on peroxide reduction or decomposition, the behavior of hydrogen peroxide on the cleavage surface of ordinary pyrolytic graphite and the edge surface of the high pressure annealed graphite was examined in helium saturated solutions containing hydrogen peroxide but no initially added O_2. The current on either surface at the most was only a few percent of the maximum values in Figs. 2 and 3 at potentials less negative than -0.50 V even with peroxide concentrations in excess of 0.1 M, which is several orders of magnitude greater than that present in measurements made without added peroxide.

The reduction of O_2 also has been examined on these graphite surfaces in O_2-saturated solutions containing from 0.0003 to 0.07 M hydrogen peroxide. The addition of the hydrogen peroxide, however, produced a small decrease rather than an increase in the cathodic current at potentials less negative

than -0.50 V (see e.g., Fig. 8). The effect was found to increase with increasing peroxide concentration. Furthermore for a given peroxide concentration the effect was very small upon first addition of the peroxide and became greater when the voltage scans were repeated several times. This indicates that the peroxide modifies the surface properties of the graphite even when present at only low concentrations (e.g., $\approx 10^{-3}$ M). At more negative potentials than -0.6 V the current was substantially increased because of peroxide reduction (compare Fig. 8 with Fig. 2).

On the basis of the experiments in peroxide containing solution both with and without O_2 saturation, it does not appear that the small difference between experimental and calculated diffusion limiting current arises from peroxide reduction or decomposition. The possibility that some small fraction of the O_2 is reduced to water without peroxide as an intermediate can not be disproved on the basis of the present experiments. Prior analytical experimentals with various graphite and carbon electrodes of larger area in the authors' laboratory, however, have indicated that the reduction of oxygen proceeds quantitatively to peroxide in alkaline solutions at the low peroxide concentrations involved in the present work. Direct four-electron reduction of O_2 to water might occur on traces of platinum deposited on the graphite, however, but such an explanation is rather questionable.

Supersaturation of the solution with O_2 may have occurred because of the whipping of small bubbles into the solution during the operation of the rotating disc electrode. For example, bubbles of 10 microns diameter can lead to supersaturation in excess of 20%. This effect alone could readily explain the small difference in experimental and calculated B' values in Table I. In any event, the difference is sufficiently small so as not to disturb the interpretation of the O_2 electrode kinetics significantly.

The hysteresis evident in the cathodic studies (Figs. 2,3,8) is apparently caused by a slow change in the state of the electrode surface at various potentials. The effect is more pronounced when the voltage scan extends to potentials quite anodic to the open circuit value. A small difference persists at open circuit even in peroxide containing solutions (Fig. 8). This suggests that the open circuit potential is under mixed control. While one of the couples is undoubtedly O_2-HO_2^-, the second couple must have a reversible potential at more negative potentials than the O_2-HO_2^- couple since the rest potentials are slightly cathodic (by 10 to 20 mV) to the calculated reversible potential for the O_2-HO_2^- couple. The only possibility is some couple associated with the oxidation of the graphite.

In Figs. 9 and 10 are plots of the potential vs the function log $[i/(i_L-i)]$ for the current-potential data given in Figs. 2 and 8 with i_L taken as the maximum current or value corresponding to the plateau. The data for ordinary pyrolytic graphite in Fig. 3 yield a plot virtually identical to that for the high pressure annealed material in Fig. 9. The function log $[i/(i_L-i)]$ will be shown later to be the appropriate function for such plots when a limiting current corresponding to diffusion or kinetic control or combined diffusion-kinetic control are involved. These plots are linear over up to two decades and have slopes of -0.11 V/decade in 1 M KOH without any peroxide added and -0.14 V/decade in 1 M KOH + 0.047 M H_2O_2, both virtually independent of rotation rate.

The pH dependence of the cathodic current at a constant potential against an external reference electrode has been examined on the edge orientation of the high pressure annealed graphite by adding given amounts of concentrated sulfuric acid to the oxygen saturated 1 M KOH solution at time intervals of 60 to 90 sec at a constant rotation rate. A steady state current was achieved within

---

[d] Based on a standard reduction potential[3] of E_o = -0.048 V at 25°C.

30 to 60 sec after each addition of acid. Over the pH range 14 - 9.7 the cathodic currents decreased by less than 50% at a potential of -0.4 V re Hg/HgO, 1 M KOH. The interpretation of this small change is complicated by changes in junction potential and oxygen solubility. Such a small change corresponds to an apparent reaction order of less than 1/10 and probably reflects changes in the state of ionization of acid and alkaline organic groups on the edge surface. The reaction order with respect to OH^- will be taken as zero under these conditions. Since the dissociation constant[14] of H_2O_2 is 2.4×10^{-12}, the pH studies did include the range over which the product of the cathodic reduction shifts from the perhydroxide ion HO_2^- to undissociated H_2O_2.

The reduction of oxygen on the cleavage surfaces of the single crystal graphite and high pressure annealed graphite (Fig. 11) proceeds far slower than on the edge orientation of the high pressure annealed pyrolytic graphite or the cleavage surface of ordinary graphite. The voltage-current curves for the cleavage surface of the high pressure annealed graphite, however, have a shape similar to that for the edge orientation (see Fig. 2) and yield a value of $\partial E/\partial \log[i/(i_L-i)] = \sim -0.10$ V/decade (see Fig. 10). Even though the currents in Fig. 11 are very small compared to the diffusion limiting values for O_2, the curves are still sensitvie to stirring. This suggests that the sites at which O_2 reduction is proceeding are separated by distances comparable to or larger than the Nernst diffusion layer thickness and hence that appreciable concentration gradients are set up about these sites. These sites are probably at imperfections in the cleavage surface where the edge orientation is exposed. The even lower current densities found for the reduction of O_2 on the cleavage surface of the single crystal are in accord with this explanation since this surface should be much closer to perfect than that of the high pressure annealed graphite.

The edge and cleavage orientations of the high pressure annealed pyrolytic graphite have also been examined cathodically after anodic pretreatment at 2.0 V in O_2-saturated 1 M KOH. The oxygen reduction curve is essential unchanged on the edge orientation. On the cleavage surface the oxygen reduction is no longer inhibited and the reduction curve is similar to that on the edge orientation. The anodic pretreatment apparent attacks the cleavage surface and may expose edges of the graphite planes.

The anodic oxidation of HO_2^- on the cleavage surface of ordinary pyrolytic graphite and the edge surface of high pressure annealed pyrolytic graphite is characterized by a large hysteresis effect (see Figs. 12 and 13) and generally poor reproducibility. A change in the surface of the graphite appears to occur at these anodic potentials and to lead to a substantial decrease in the rate constant for the peroxide oxidation. The tendency for the current-potential curves to plateau on the first sweep in the anodic direction in Figs. 12 and 13 may correspond to a limiting current or may reflect the offsetting of the increment in current with increasing potential by the decrease of the activity of the surface withtime. After several sweeps with increasing and decreasing anodic potentials, the curves showed no indication of a plateau and relatively little further change provided the sweep rate was held constant and not interrupted.

A comparison of Figs. 12 and 13 indicates that the anodic oxidation both in the initial anodic sweeps and subsequent sweeps is substantially more reversible for the edge surface of the high pressure annealed graphite than for the cleavage surface of ordinary graphite. This is in contrast to the cathodic behavior for which the reversibility is almost the same on both of these surfaces. On the cleavage surface of the high pressure annealed pyrolytic graphite the anodic current is extremely small (Fig. 12), amounting to only $\sim$0.08 mA/cm^2 at +0.5 V on repeated sweeps with either increasing or decreasing anodic potentials.

Despite the poor reproducibility of the anodic measurements, plots of log i vs potential after several sweeps to anodic potentials of 0.5 V re Hg/HgO, 1 M KOH have been made for various peroxide concentrations (0.015 to 0.18 M) and found to exhibit linearity over 1 to 1.5 decades. The slopes scatter substantially from run to run, however, and fall in the range 0.22 to 0.26 V/decade and occasionally as high as 0.30 V/decade.

The lack of reproducibility in the anodic measurements precluded the determination of the dependance of the exchange current and transfer coefficient on peroxide and OH^- concentration. An attempt was made to determine the reaction orders, however, in the same manner as used in the cathodic studies by adding peroxide or sulfuric acid at a constant potential relative to the Hg/HgO, 1 M KOH reference electrode and constant rotation rate. Over the peroxide concentration range 0.00065 to 0.15 M HO_2^- in solutions formed by adding concentrated H_2O_2 to 1 M KOH the reaction order was 0.9 or approximately 1 at a potential of +0.20 V. Dilution effects were negligible and hence the OH^- concentration decreased only by the amount used to compensate the ionization of the H_2O_2 to form HO_2^-.

The dependence of the oxidation current on pH was examined at a potential of 0.3 V by adding concentrated sulfuric acid to a solution containing initially 1 M KOH plus 0.078 M H_2O_2. The results are shown in Fig. 14 together with the dependence of i on pH to be expected if the kinetics follow an equation of the form

$$i = k[HO_2^-] = kK[H_2O_2]\,[OH^-] \qquad (2)$$

where the bracketted quantities are the molar concentrations and

$$K = \frac{[HO_2^-]}{[H_2O_2]\,[OH^-]} = 10^{2.3}\ \underline{M}^{-1} \qquad (3)$$

and k is the effective first order rate constant. The pH dependence at pH above 12 approximates closely the behavior predicted by eq. (2) but at lower

pH the experimental data deviate by a large amount. No single set of reaction orders for $[OH^-]$, consistent with either HO_2^- or H_2O_2 as the reactant, fits the observed pH dependence. This implies that either a change in reaction mechanism or rate determining step occurs at lower pH or the state of ionization of various organic groups bound to the surface changes or both.

The only conclusions which can be drawn from the anodic studies are that after several sweeps the oxidation is characterized by a quite high Tafel slope and is first order with respect to HO_2^- and correspondingly zero order with respect to OH^- at pH > 12.

DISCUSSION OF MECHANISMS

The inhibition of oxygen reduction and peroxide oxidation on the cleavage surface of this high pressure annealed pyrolytic graphite and single crystal graphite relative to the edge orientation may be produced by any of the following:

1. differences in the electrocatalytic properties of the surfaces,

2. a much larger ratio of true-to-apparent area on the edge orientation,

3. preferential adsorption of some interfering agent on the cleavage surface,

4. preferential adsorption of some species or impurity on the edge orientation which catalyzes the oxygen-peroxide reaction.

To help differentiate between these possible explanations, the behavior of the ferri-ferrocyanide couple has been examined on these surfaces with the rotating disc technique in a 0.005 M $K_3Fe(CN)_6$ + 0.005 M $K_4Fe(CN)_6$ solution with 0.5 M K_2SO_4 as the supporting electrolyte at pH 3. The current-voltage data are presented in Fig. 15. The apparent exchange current densities $(i_o)_a$ for the edge and cleavage surfaces have been calculated from the polarization resistance $(\partial\eta/\partial i)_o$ at the reversible potential by means of the equation

$$\left(\frac{\partial \eta}{\partial i}\right)_o = \frac{RT}{F}\left(\frac{1}{(i_o)_a} + \frac{1}{(i_D)_a} + \frac{1}{(i_D)_c}\right) \qquad (4)$$

where η is the overpotential and $(i_D)_a$ and $(i_D)_c$ are the observed anodic and cathodic diffusion limiting current densities. Table II summarizes the various values used in this calculation. The apparent exchange current density for the edge surface is approximately three fold greater than on the cleavage surface of the high pressure annealed pyrolytic graphite.

TABLE II. Parameters involved in the calculation of the apparent exchange current densities for the ferri-ferrocyanide redox couple on the cleavage and edge surfaces of high pressure annealed pyrolytic graphite.

	$(\partial\eta/\partial i)_o$ (ohm-cm^2)	$(i_D)_a$ (mA/cm^2)	$-(i_D)_c$ (mA/cm^2)	$(i_o)_a$ (mA/cm^2)
edge	20	4.2	4.9	3.0
cleavage	34	3.9	4.5	1.1

This difference in apparent exchange current density may be caused by a difference in the ratio of true-to-apparent area but this difference would be too small to explain the 15 fold difference in the oxygen reduction current densities and 50 fold difference in the peroxide oxidation current densities. The difference in the exchange current densities for the ferri-ferrocyanide couple on the two orientations is more likely due to a difference in the ionic double layer on the two surfaces arising from the presence of polar ionizable groups on the edge orientation and the lack of such on the cleavage surface. Double layer effects would be expected to be large with the ferri-ferrocyanide couple even with a high concentration of supporting electrolyte because of the high charge of the redox reactants. With the oxygen reduction, however, double layer effects in the presence of a supporting electrolyte should be small.

Differential capacitance measurements have been made on the two orientations at 1000 Hz and indicate values of 71.5 $\mu f/cm^2$ and 28.6 $\mu f/cm^2$ for the edge and cleavage surfaces of the high pressure annealed pyrolytic graphite respectively, and 10.3 $\mu f/cm^2$ for the cleavage surface of the single crystal, all at a potential of -0.300 V re Hg/HgO, 1 M KOH in helium saturated 1 M KOH. The ratio of the capacities on the edge and cleavage surfaces of the high pressure annealed pyrolytic graphite is approximately 2.6 fold or almost the same as the ratio of the apparent exchange current densities for the ferri-ferrocyanide redox couple. This may reflect the fact that both the exchange current densities and the differential capacity of the interface are proportional to the true surface area. It is more likely, however, that the closeness of these two ratios is coincidence since the differential capacity should depend on the intrinsic structure of the interface as well as the true area and hence should differ for the edge and cleavage orientations even if both had the same true area.

The relatively low value of the differential capacitance for the cleavage surface of the single crystal may be caused by some contribution from the space charge within the graphite. The organization of the solution side of the interface also may differ from that normally encountered with metal electrodes because of the hydrophobic nature of the electrode surface resulting from the satisfying of the surface valencies in the plane of the electrode surface.

The authors believe that the difference in the behavior of the oxygen-peroxide couple on the two orientations reflects the difference in electrocatalytic properties of the two orientations. These two surfaces should exhibit marked differences in their ability to adsorb reactants and intermediates in the oxygen-peroxide reactions. A reasonable conjecture is that the edge orientation adsorbs reactants and/or intermediates thus providing the strong interaction of the electrode phase with solution phase species necessary for the reaction to proceed at a reasonable rate while the cleavage surface does not.

The possibil.ty that some foreign species such as platinum is adsorbed preferentially on one of the orientations and effects the kinetics of the oxygen-peroxide couple can not be completely disproved on the basis of the present work. The insensitivity of the results to pre-electrolysis with platinum electrodes, however, is evidence against such an explanation for the difference in the behavior of the oxygen peroxide couple on the two orientations. Furthermore the cathodic behavior of the O_2-peroxide couple on the edge orientation is essentially the same as observed in earlier studies[3,15] or ordinary graphite without pre-electrolysis and with graphite or carbon counter electrodes--thus presenting no opportunity for platinum contamination of the electrodes or solution.

For the oxygen reduction on the edge orientation, the reduction of oxygen to peroxide is first order in O_2 concentration and essentially zero order in OH^- and H_2O_2 or HO_2^- concentration and has a value for the apparent transfer coefficient of 0.5[4] or approximately 1/2. The large differences in the reversibility of this couple on the two different orientations and also on various metals is evidence that the reduction proceeds at a substantial rate only through a strong interaction with the electrode surface and not the type of charge transfer discussed by Marcus[16] for certain redox couples for which the transition state does not involve strong interaction between orbitals of the redox species and those of the electrode. While the number of electrons involved in the rate determining step might be two, this appears unlikely since the simultaneous transfer of two electrons usually results in far too high an energy of activation. Thus the transfer coefficient α for the rate determining step is most likely 1/2. Furthermore the rate determining charge transfer step probably is the first electron transfer in the reduction of the O_2 rather than the second. An apparent transfer coefficient of 1/2 could be found with the second electron transfer as rate determining only if the fraction of the surface sites covered by the adsorbed intermediate which is the reactant for

this step is large. This seems rather unlikely with any of the intermediate species which would be expected in the oxygen reduction to peroxide without bond cleavage.

An examination of Figs. 2, 3, 6, 7, and 8 indicates that the current density corresponding to pure kinetic control (i_k) in eq. (1) passes through a maximum or a plateau with increasing cathodic potentials. This probably means that a step which is to a first approximation potential independent is involved in the reduction of O_2 to peroxide. The current then may decrease somewhat at more cathodic potentials after passing through the maximum because of secondary effects associated with a decrease in the electrocatalytic activity of the electrode surface. At even more cathodic potentials the overall current again increases probably because of peroxide reduction and/or direct reduction of O_2 beyond the peroxide state. An alternative but less likely explanation is that the maximum or plateau may be caused entirely by a very substantial decrease in the electrocatalytic activity of the surface which offsets or more than offsets the usual increase of the rate of the charge transfer processes with increasing potential.

An attempt has been made to evaluate the stoichiometric number from the current-potential data for the reduction of O_2 in solutions containing HO_2^- (Fig. 8). The apparent exchange current density $(i_o)_a$ was determined from the intercept with the abscissa in Fig. 10 with the equation

$$\eta = -\frac{RT}{\alpha F}\left[\ln \frac{i}{i_L - i} - \ln \frac{(i_o)_a}{-i_L}\right] \qquad (5)$$

where i_L is the current density[e] corresponding to the observed plateau in the current-voltage curve. Equation (5) is valid when charge transfer is partially

---

[e] In this paper, cathodic currents (including i_L) are taken as negative and anodic currents as positive.

rate controlling with the back reaction negligible and the observed limiting current is caused by either mass transport control or a potential insensitive chemical step, or both with the kinetics first order with respect to the diffusing reactant. The stoichiometric number ν has been calculated from the activation polarization resistance $(\partial\eta_a/\partial i)$, evaluated at $\eta = 0$, by means of the equation

$$\left(\frac{\partial\eta_a}{\partial i}\right)_o = \left(\frac{\partial\eta}{\partial i}\right)_o - \left(\frac{\partial\eta_d}{\partial i}\right)_o = -\frac{RT}{F}\cdot\frac{1}{(i_o)_a}\cdot\frac{\nu}{n} \qquad (6)$$

where $(\partial\eta/\partial i)_o$ and $(\partial\eta_d/\partial i)_o$, are the overall polarization resistance and the concentration polarization resistance, respectively, and n is the overall number of electrons per mole of O_2 $(n = 2)$. This equation involves the assumption that only one step is rate controlling (e.g., charge transfer). Furthermore in using $(i_o)_a$ from eq. (5) in eq. (6), the additional assumption is made that the $(i_o)_a$ is constant over a potential range extending from $\eta = 0$ through the linear region of the $-\eta$ vs $\log [i/(i_L - i)]$ plots in Fig. 10. The concentration polarization resistances have been calculated by means of the equation:

$$\left(\frac{\partial\eta_d}{\partial i}\right)_o = -\frac{RT}{nF}\,\frac{1}{i_D} \qquad (7)$$

where the diffusion limiting current density has been obtained from the slopes of the plots in Fig. 7. Mass transport of peroxide can be neglected in view of its high concentration.

The values of the stoichiometric number listed in Table III are consistently higher than 2 but provide evidence favoring 2. This deviation is not surprising since the assumption that the activation polarization involves only charge transfer as rate controlling is not fully valid if the plateaus in Figs. 8 and 12 are caused by a limiting chemical step.

The following mechanism for O_2 reduction to peroxide is compatible with the experimental data:

TABLE III. Parameters[1] involved in the determination of the apparent stoichiometric number (ν) for the reduction of O_2 in O_2-saturated (0.97 atm) solution containing 1 M KOH + 0.047 M H_2O_2 at 22°C (based on Figs. 8 and 10).

scan direction	f (rpm)	$\partial\eta/\partial\log[i/(i_L-i)]$ (V/decade)	$-I_L$ (mA)	$-i_D$(exp) (mA/cm^2)	$(i_o)_a$ (mA/cm^2)	$(\partial\eta/\partial i)_o$ (V cm^2/mA)	$(\partial\eta_d/\partial i)_o$ (V cm^2/mA)	$(\partial\eta_a/\partial i)_o$ (V cm^2/mA)	apparent ν	$(\partial\eta_a/\partial i)_o$(calc.[2]) (V cm^2/mA)
-	1200	0.12_9	0.27_7	1.7_5	0.19	0.17	0.0073	0.16	2.4	0.15
+	1200	0.12_9	0.24_2	1.7_5	0.17	0.18	0.0073	0.17	2.3	0.16
-	3600	0.12_5	0.41_2	3.0_2	0.21	0.15	0.0042	0.14	2.3	0.14
+	3600	0.12_4	0.38_1	3.0_2	0.19	0.17	0.0042	0.16	2.4	0.15

[1] I_L observed limiting current, i_D(exp) diffusion limiting current density obtained from slopes in Fig. 7, $(\partial\eta_d/\partial i)_o$ concentration polarization resistance at $\eta = 0$, $(\partial\eta_a/\partial i)_o$ activation polarization resistance at $\eta = 0$.

[2] Calculated by means of eq. (10).

Step I. $O_2 \rightarrow O_2(ad)$

Step II. $O_2(ad) + HOH + e \rightarrow HO_2(ad) + OH^-$

Step III. $2\ HO_2(ad) + OH^- \rightarrow HO_2^- + O_2 + HOH$

This mechanism does not involve O-O bond rupture, has a stoichiometric number of 2, and is first order in O_2 concentration and zero order in OH^- and HO_2^-. Step II has been written in the form shown rather than in the form $O_2(ad) + e^- \rightarrow O_2^-(ad)$ since the observed Tafel slopes correspond to an apparent transfer coefficient of 0.5. If charged specifically adsorbed species were involved in the rate-determining charge transfer step, the observed transfer coefficient would be expected to deviate substantially from this value[f] for an one-electron charge transfer step.

Step III may proceed through several separate steps involving desorption and ionization of H_2O_2. It is unlikely, however, that HO_2 or O_2^- are first desorbed and then react together in the solution phase immediately adjacent to the electrode at any appreciable rate. On the basis of Latimer's estimates[14] of the free energies of formation of these species in aqueous solutions, the standard reduction potentials for the following reactions are

$$O_2 + e \rightarrow O_2^- \qquad E^\circ = -0.56\ V$$

$$O_2 + HOH + e \rightarrow HO_2 + OH^- \qquad E^\circ = -0.96\ V$$

---

f Gnanamuthu and Petrocelli[17] have listed Tafel slopes for various reaction mechanisms with the assumption that adsorbed species are in an inner Helmholtz plane at a potential corresponding to one half the potential drop between the metal and the outer Helmholtz plane. This assumption is difficult to accept. The point is well made, however, that the apparent transfer coefficient should not be 0.5 under these circumstances since the fraction of the potential drop driving the charge transfer step is considerably less than that when the charged reacting species are in the outer Helmholtz plane.

At the standard reduction potential of the O_2-peroxide couple[3] ($E^\circ = -0.04_8$ V) the concentrations of O_2^- and HO_2 would not exceed $10^{-8.5}$ M and 10^{-15} M, respectively. These concentrations are far too low to support any appreciable current density through a homogeneous second-order diffusion controlled reaction in the Nernst layer adjacent to the electrode. At potentials several tenths of a volt more cathodic, the concentration of O_2^- might reach a value where the homogeneous diffusion controlled reaction $2\ O_2^- + H_2O \rightarrow O_2 + HO_2^- + OH^-$ occurs at an appreciable rate. To be compatible with the experimental results, however, the reaction would need to occur almost entirely within a distance from the electrode small compared to the Nernst layer. Otherwise, less than two electrons would be realized per O_2 molecule transported through the Nernst layer, which is contrary to observation.

The reduction mechanism has been written with the adsorption of O_2 as the first step on the basis that such a potential insensitive step might become rate controlling at high currents and provide an explanation for the maximum in i_k. Alternatively, if the fraction of available sites for HO_2 which are occupied at more cathodic potentials approaches unity, Step III might also give rise to a maximum in i_k. This seems less likely for a species as reactive as HO_2 and furthermore it is questionable if the reduction would be a linear function of $\log [i/(i_L-i)]$.

Evidence for an adsorption step preceeding the charge transfer step is to be found in the reversible chemiadsorption of O_2 on carbon from the gas phase, presumedly without bond cleavage, as revealed by electron spin resonance studies[18]. Both the line width and integrated peak height for the unpaired delocalized electrons in the carbon are changed during the O_2 adsorption probably because the adsorption involves an interaction with these unpaired electrons and leads to their localization at surface sites.

The current-overpotential relationship corresponding to the mechanism

represented by Steps I-III is

$$-i = (i_o)_2\left[\frac{i_a - i}{i_a}\exp -\frac{\alpha_2 Fn}{RT} - \left(\frac{i_b - i}{i_b}\right)^{1/2}\exp\frac{(1-\alpha_2)Fn}{RT}\right] \qquad (8)$$

where $(i_o)_2$ and α_2 are the apparent exchange current density and transfer coefficient for Step II and

$$\frac{1}{i_a} = -\frac{1}{(i_o)_1} + \frac{1}{i_D} \quad \text{and} \quad \frac{1}{i_b} = \frac{1}{(i_o)_3} + \frac{1}{i_D} \qquad (8a,b)$$

where $(i_o)_1$ and $(i_o)_3$ are the apparent exchange current densities for Steps I and III, respectively, and i_D is the diffusion limiting current density for O_2 based on two electrons/O_2. Note[e] that i_b is positive and that i_a and i_D are negative; the exchange current densities have no sign. The peroxide concentration has been taken to be high compared to that of O_2. Further assumptions are that the surface coverage with adsorbed O_2 and HO_2 are small and that Step III is relatively potential independent.

For eqs. (8a,b) to be applicable under anodic conditions, it must be possible to achieve supersaturation of the solution adjacent to the electrode with O_2 by a factor[e] of $[1-(i/i_D)]$ without bubble formation relieving this supersaturation to any appreciable extent. For the anodic current density corresponding to the plateau in Fig. 12, this requires supersaturation by a factor of ~4.5 fold. Far greater supersaturation has been achieved in other studies[19] involving H_2 discharge on a rotating platinum disc electrode without bubble formation over the surface of the electrode.

For the cathodic branch at sufficiently negative values of n, eq. (8) reduces to eq. (5) where $i_a = i_L$ and $(i_o)_2 = (i_o)_a$. For values of n such that $|Fn/(RT)| << 1$, eq. (8) reduces to

$$\frac{\partial n}{\partial i} = \frac{\partial n_a}{\partial i} + \frac{\partial n_d}{\partial i} \qquad (9)$$

where $\partial n_d/\partial i$ is given by eq. (7) with n = 2 but $\partial n_a/\partial i$ is now

$$\left(\frac{\partial n_a}{\partial i}\right)_o = -\frac{RT}{F}\left[\frac{1}{(i_o)_1} + \frac{1}{(i_o)_2} + \frac{1}{2(i_o)_3}\right] \qquad (10)$$

Thus $(i_o)_a$ in eq. (6) corresponds to the bracketted quantity on the right side in eq. (10) with $\nu/n = 1$ whereas $(i_o)_a$ in eq. (5) corresponds to $(i_o)_2$.

The validity of eq. (10) can be checked at least approximately with cathodic and anodic data of the type represented in Figs. 8 and 12 for the edge orientation of high pressure annealed pyrolytic graphite in O_2-saturated solutions of moderately high peroxide concentration. The application of eq. (8a) to the current-rotation rate data in Fig. 8 at a potential of -0.5 V re Hg/HgO, 1 M KOH yields $(i_o)_1 = 5.7$ mA/cm^2 for sweeps in the cathodic direction and 4.6 mA/cm^2 for sweeps in the reverse direction or ~5 mA/cm^2. Likewise from the first sweep in the anodic direction in Fig. 12, i_b is 6.0 mA/cm^2. With this value and that for $i_D = -1.75$ mA/cm^2 at 1200 rpm (see Table III) eq. (8b) gives $(i_o)_3 = 1.35$ mA/cm^2. The values for $(\partial\eta_a/di)_o$ - calc. listed in the last column in Table III have been calculated with eq. (10) using these values for $(i_o)_1$ and $(i_o)_3$ and, values for $(i_o)_a$ in this same table. The comparison of the calculated and observed values for $(\partial\eta_a/di)$ is quite favorable. The terms involving $1/(i_o)_1$ and $1/[2(i_o)_3]$ in eq. (10) also explain why the stoichiometric numbers calculated by means of eq. (6) were consistently high by 10 to 20%.

Unfortunately the large amount of hysteresis and general lack of reproducibility encountered in the anodic studies of the O_2-peroxide couple prevent a reliable test of whether the mechanism represented by Steps I-III is followed in reverse for the oxidation peroxide to O_2. Just on the chance that the cathodic mechanism might be followed in reverse on the first anodic sweep, the data in Fig. 12 were plotted in terms of E vs. log $[i/\sqrt{i_b - i}]$. Some indication of linearity was found at $n >> RT/F$ but this linearity extended only over a decade and the slope was 0.27 V/decade, a value far too high to be complementary to the observed cathodic slopes for $\nu = 2$ or for that matter any integer value. Plots of η vs log $[i/(i_b - i)]$ for the first anodic sweep also are relatively linear over a decade with a slope of 0.22 V/decade.

The anodic behavior after a number of sweeps in either direction also does not match up with eq. (8). No limiting currents are evident and the Tafel plots

(log i vs E) exhibit linearily over 1.5 to 2 decades but the slopes are high and not reproducible (0.22 - 0.30 V/decade). The reaction orders of ~1 for HO_2^- and 0 for OH^- do not match up with those expected for the reverse of Steps I-III with Step II rate controlling. Much of the difficulty is believed to arise because of progressive changes in the state of oxidation of the graphite surface at these anodic potentials. At this time, little can be concluded as to the mechanism for peroxide oxidation on pyrolytic graphite.

It is interesting to note, however, that the observed reaction orders for HO_2^- and OH^- do coincide with those for the reverse of Step III as rate controlling. Perhaps the progress changes in the surface properties at anodic potentials are such that Step III becomes rate controlling. The high Tafel slopes may correspond to some small amount of potential dependence for the rate of this step.

In the earlier studies[3,15] of the O_2-peroxide couple on paraffin-filled graphite electrodes, an anodic limiting current of a kinetic origin was observed and found to be first order in HO_2^- at concentrations from 0.11 to 0.66 M in 4 M KOH and zero order in OH^- at concentrations from 0.1 to 3.8 M with 0.3 M HO_2^- present. Furthermore plots of n vs log $[i/(i_L-i)]$ for peroxide oxidation yielded linear plots for n > RT/F with slopes of ~0.12 V/decade over 1.5 to 2 decades. In contrast the cathodic behavior of the O_2-peroxide couple on the paraffin-filled graphite was almost the same as on the edge surface of the high pressure annealed pyrolytic graphite, the principle difference being that for the paraffin-filled graphite the limiting current appeared to be entirely diffusion controlled. Further work is required to identify what chemical features of these two surfaces are responsible for the differences in the behavior of the O_2-peroxide couple on them.

The mechanism represented by Steps I-III does not reflect the chemical features of the surface. Specific chemical groups may be involved as intermediates. Future work will be directed to establishing what chemical groups are

present and what their role in O_2 electrode kinetics may be.

ACKNOWLEDGEMENT

The authors are pleased to acknowledge the help of Dr. Robert Greef, particularly in the examination of the ferri-ferrocyanide couple on the pyrolytic graphite.

REFERENCES

1. W. Berl, Trans. Electrochem. Soc. 88, 253 (1943).

2. M. Davies, M. Clark, E. Yeager, and F. Hovorka, J. Electrochem. Soc. 106, 56 (1959).

3. E. Yeager, P. Krouse, and K. V. Rao, Electrochem. Acta 9, 1057 (1964).

4. D. Maricle and W. Hodgson, Anal. Chem. 37, 1562 (1965).

5. A. Ubbelohde, D. Young, and A. Moore, Nature 198, 1192 (1963).

6. J. Nelson and A. C. Riddiford, J. Electrochem. Soc. 108, 695 (1961).

7. V. Levich, Acta Phys. Chim. URSS, 17, 257 (1952); Physico-chemical Hydrodynamics, Prentice Hall, Inc., Englewood Cliffs, N.J., 1962.

8. D. Yohe, E. Yeager, R. Greef, and A. Riga, Electrochemical Processes on Nickel Oxide, Technical Report 3, Case Western Reserve University, Cleveland, Ohio, U. S. Office of Naval Research, Contract Nonr 1439(09), 1 July 1967, pp. 137-141.

9. R. Zurilla and E. Yeager, Case Western Reserve University, Cleveland, Ohio (unpublished research).

10. J. Newman, J. Phys. Chem. 70, 1327 (1966).

11. R. Davis, G. Horvath, and C. Tobias, Electrochim. Acta 12, 287 (1967).

12. K. Gubbins and R. Walker, J. Electrochem. Soc. 112, 469 (1965).

13. J. Lingane and B. Loveridge, J. Am. Chem. Soc. 72, 438 (1950).

14. W. M. Latimer, Oxidation Potentials, 2nd edition, Prentice-Hall, N.Y., 1952.

15. K. V. Rao, Kinetics of the Oxygen Electrode, Ph.D. thesis, Case Western Reserve University, Cleveland, Ohio, 1961.

16. R. A. Marcus, J. Chem. Phys. 24, 966 (1956); 26, 867 (1957). J. Phys. Chem. 67, 853 (1963).

REFERENCES (Continued)

17. D. S. Gnanamuthu and J. V. Petrocelli, J. Electrochem. Soc. 114, 1036 (1967).

18. L. Singer and W. Spry, Bull. Am. Phys. Soc. 1 214 (1956).

19. F. Ludwig and E. Yeager, Hydrogen Overvoltage on Platinum, Technical Report 21, Case Western Reserve University, Cleveland, Ohio, U. S. Office of Naval Research Contract N00014-67-C-0389, Project NR 359-277, 1 February 1968, pp. 197-203.

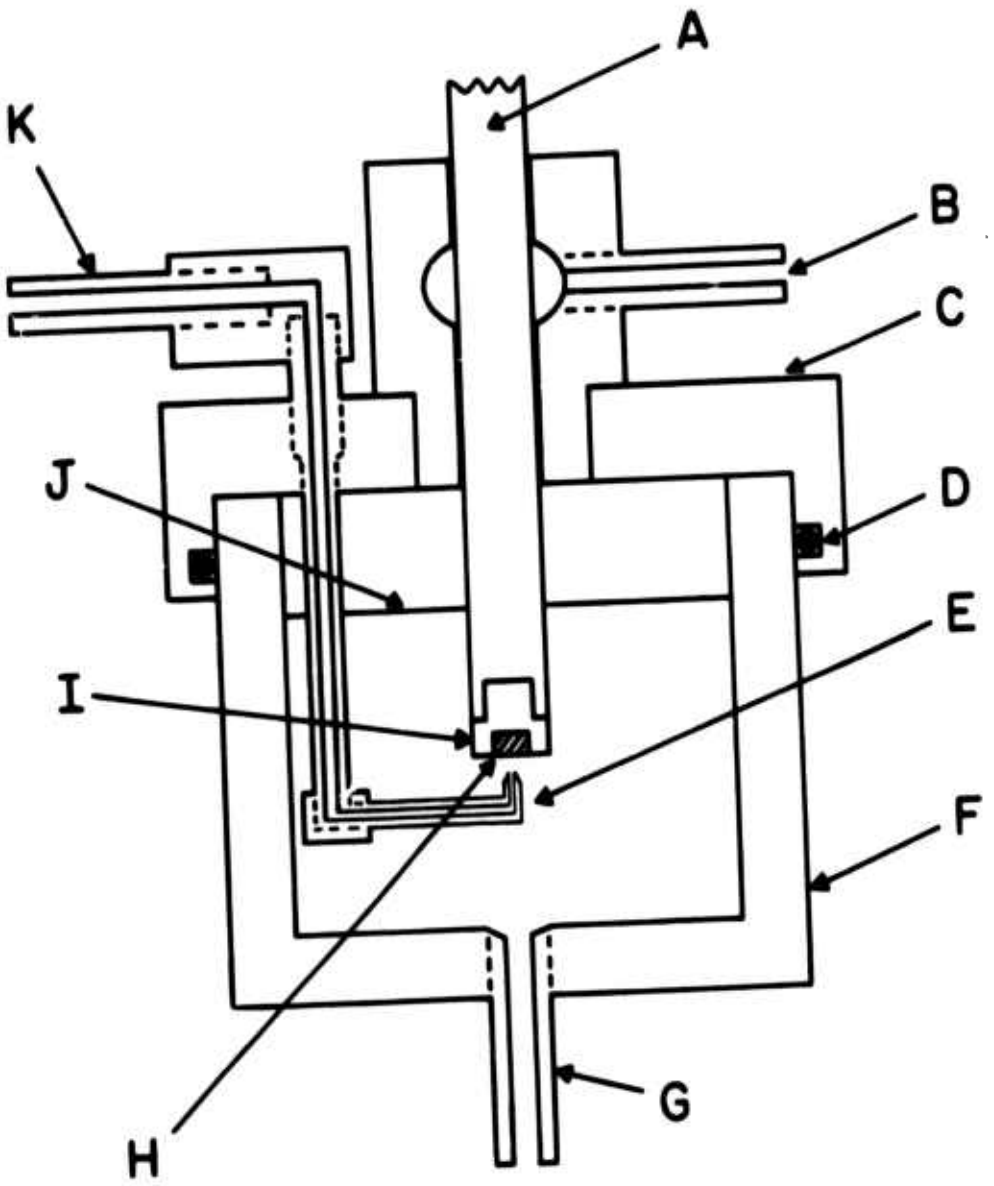

Figure 1. Electrochemical cell (counter electrode and gas saturation tube not shown). A - Teflon coated rotating steel shaft, B - gas inlet, C - Teflon cover, D - Viton O-ring, E - Luggin capillary, F - Teflon cell, G - drain tube, H - working electrode (graphite), I - Kel-F electrode mounting, J - solution level, K - connection to reference electrode.

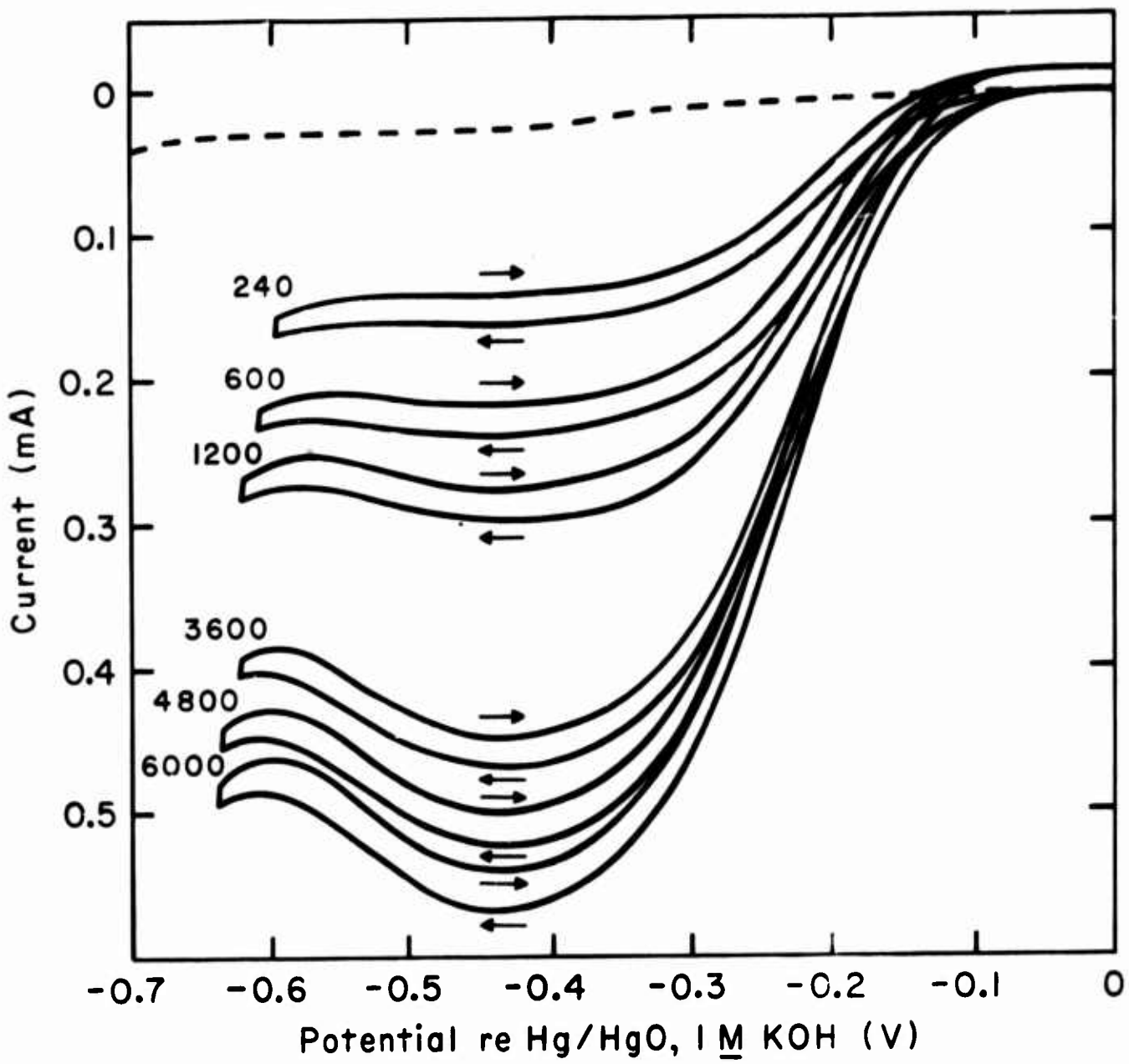

Figure 2. Reduction of O_2 on high pressure annealed pyrolytic graphite. —— edge orientation, --- cleavage orientation. Electrolyte: 1 M KOH, pressure O_2: 0.97 atm, temperature: 22°C, electrode area: 0.22 cm^2. Rotation rates indicated on curves in rpm. Direction of sweep indicated by arrows.

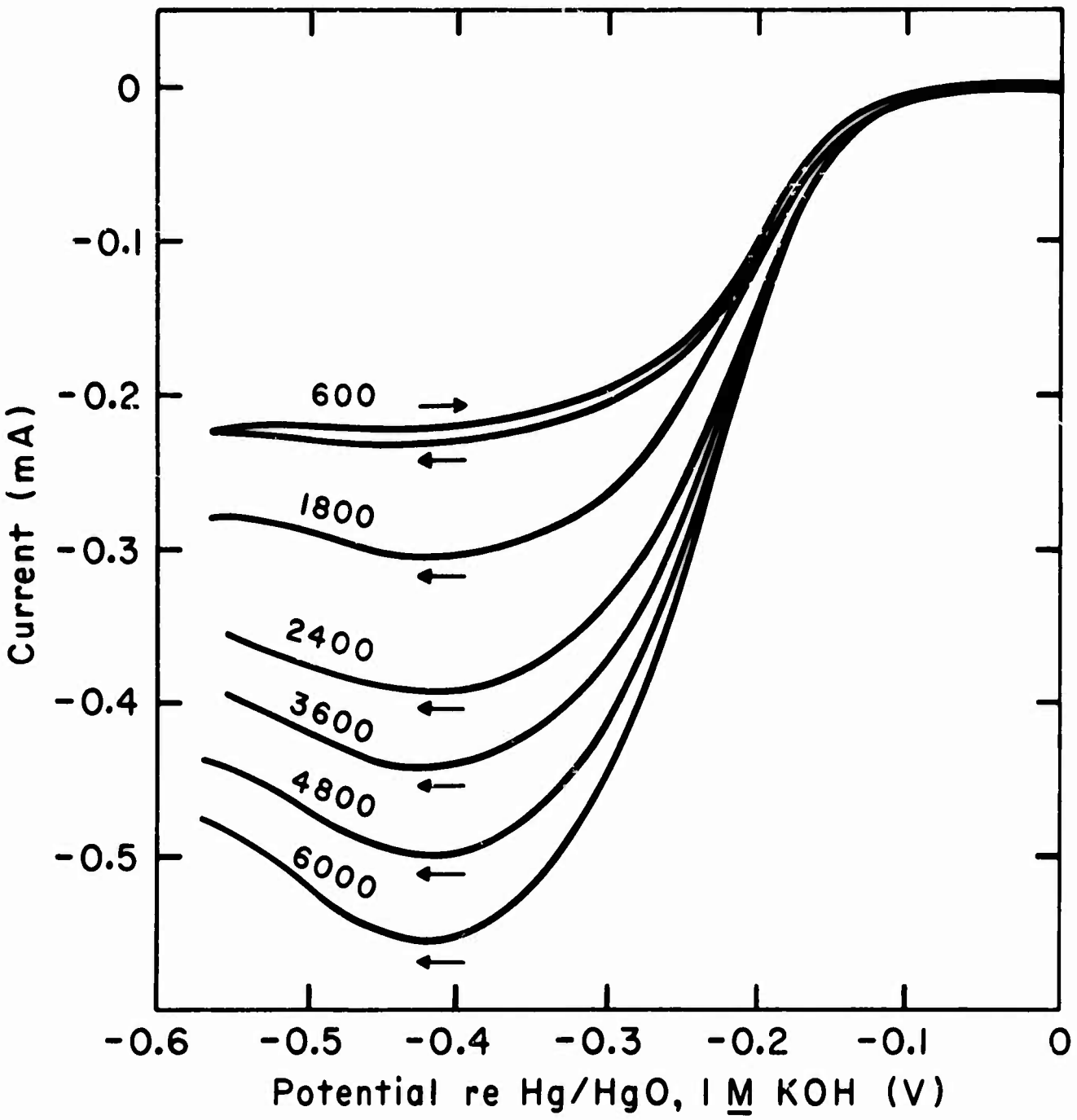

Figure 3. Reduction of O_2 on cleavage orientation of ordinary pyrolytic graphite. Electrolyte: 1 M KOH, pressure O_2: 0.97 atm, temperature: 22°C, electrode area: 0.196 cm^2. Rotation rates indicated on curves in rpm. Direction of sweep indicated by arrows.

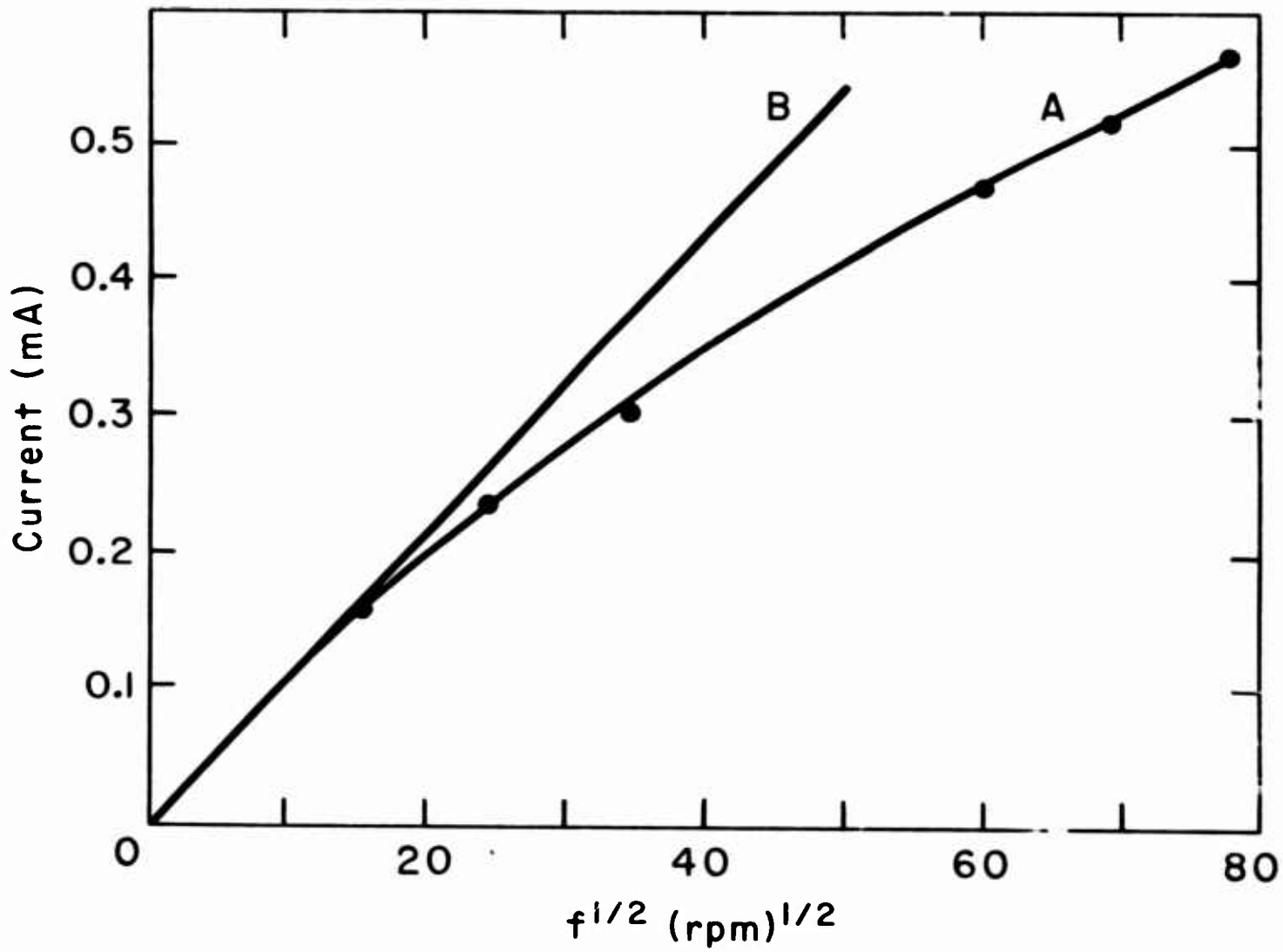

Figure 4. Reduction of O_2 on edge surface of high pressure annealed pyrolytic graphite. Electrolyte: 1 M KOH, pressure O_2: 0.97 atm, temperature: 22°C, area: 0.22 cm^2, potential: -0.43 V re Hg/HgO, 1 M KOH. Curve A: smooth curve through points obtained from Fig. 2 (sweeps in cathodic direction). Curve B: diffusion limiting current determined from slope of plot in Fig. 3.

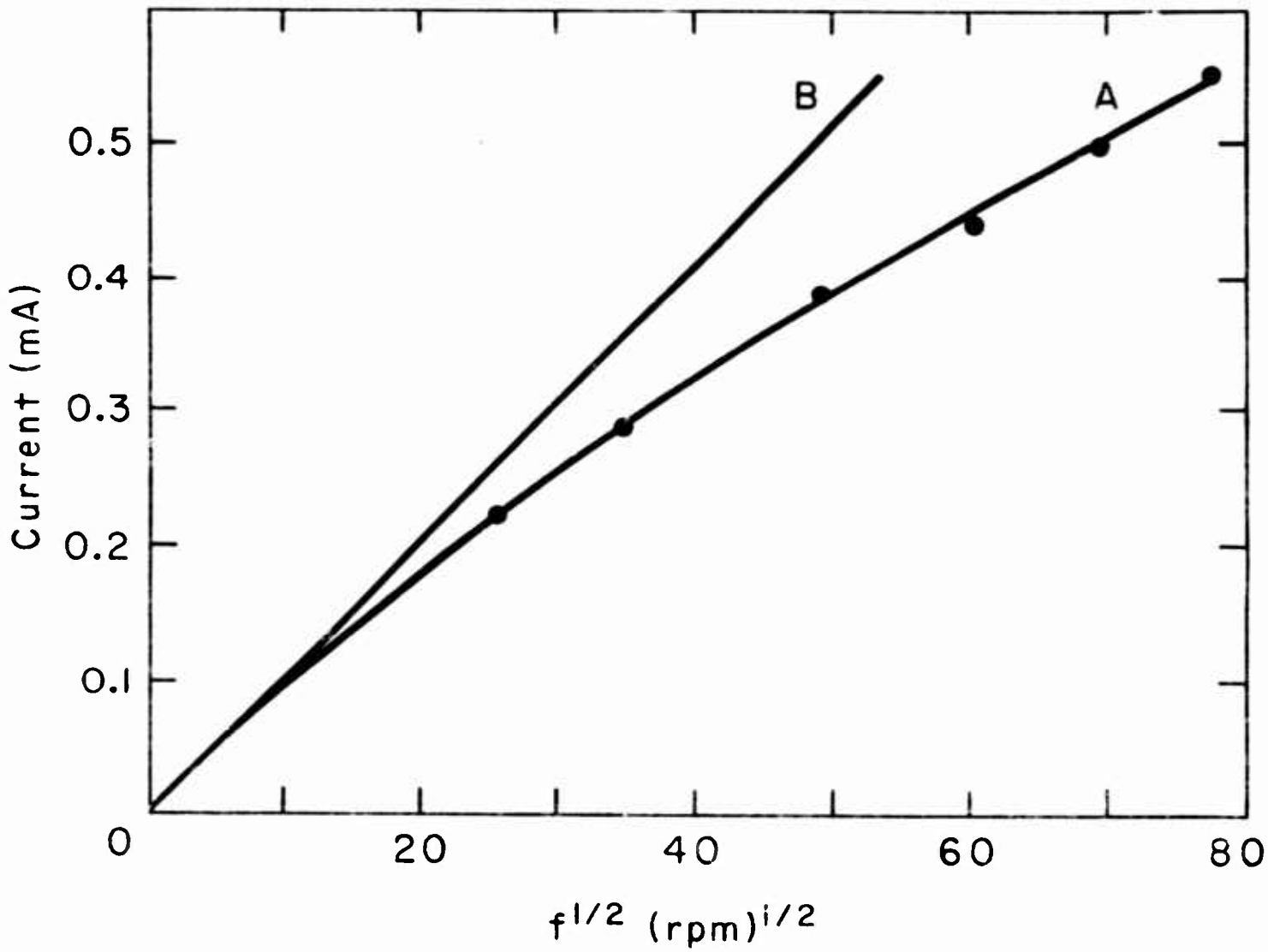

Figure 5. Reduction of O_2 on cleavage surface of ordinary pyrolytic graphite. Electrolyte: 1 M KOH, pressure O_2: 0.97 atm, temperature: 22°C, area: [illegible] cm^2, potential: -0.43 V re Hg/HgO, 1 M KOH. Curve A: smooth curve through points obtained from Fig. 3. Curve B: diffusion limiting current determined from slope of plot in Fig. 7.

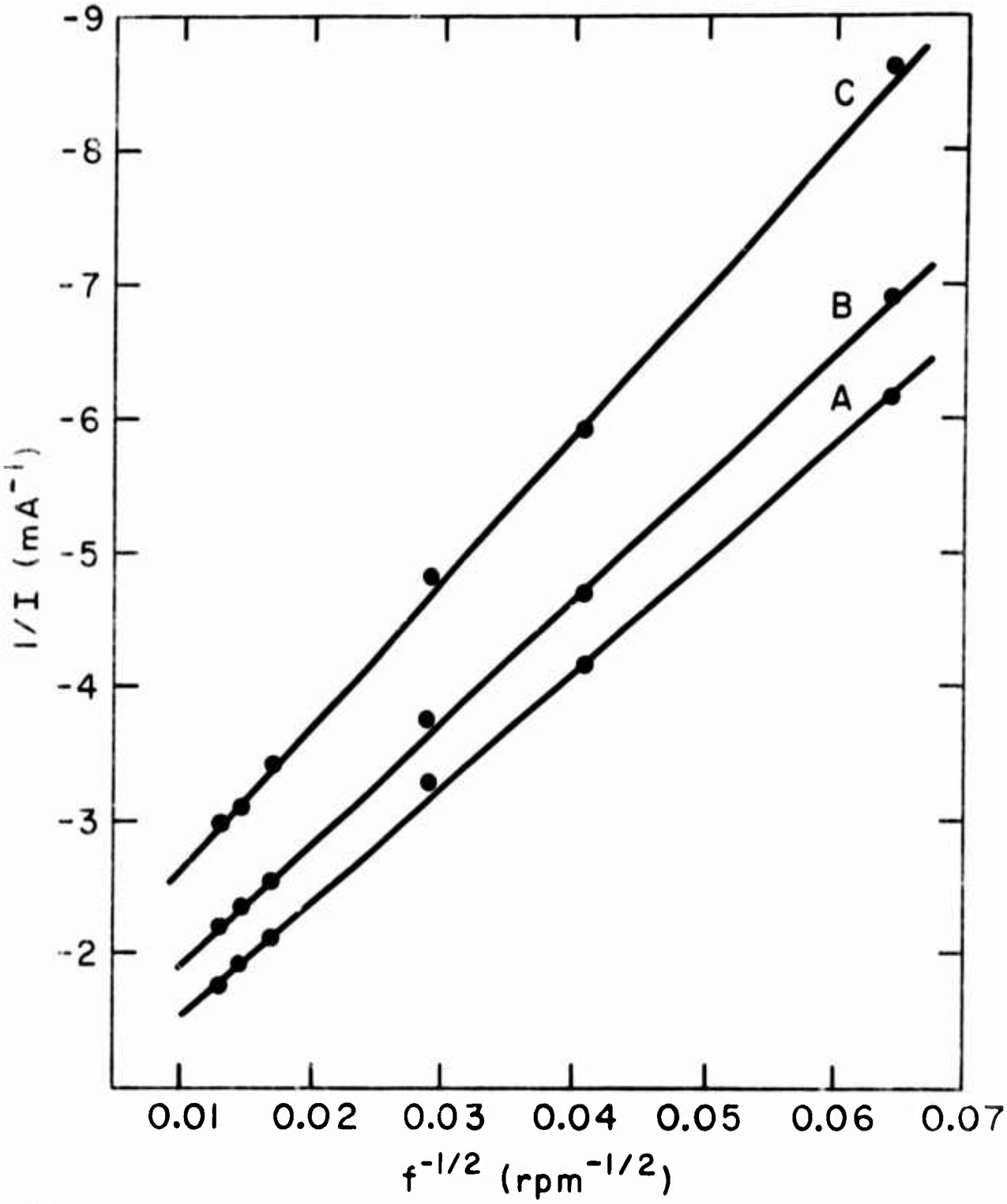

Figure 6. Reduction of O_2 on the edge surface of high pressure annealed pyrolytic graphite at fixed potentials. Electrolyte: 1 M KOH, pressure O_2: 0.97 atm, temperature: 22°C, area: 0.22 cm^2. Curve A: -0.43 V re Hg/HgO, 1 M KOH, Curve B: -0.30 V, Curve C: -0.25 V.

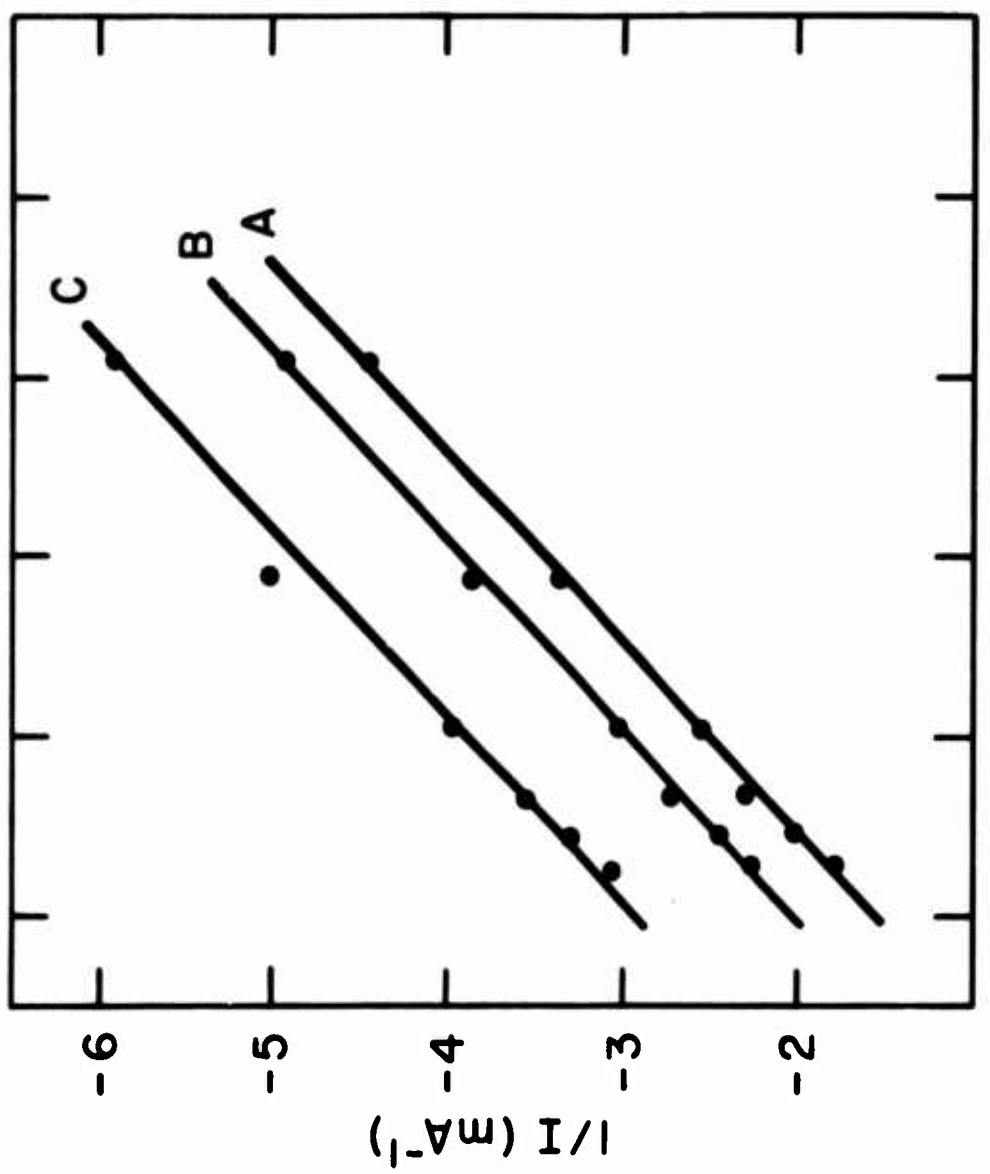

Figure 7. Reduction of O_2 on cleavage surface of ordinary pyrolytic graphite at fixed potentials. Electrolyte: 1 M kOh, pressure O_2: 0.97 atm, temperature: 22°C, area: 0.196 cm^2. Curve A: -0.30 V, Curve B: -0.35 V, Curve C: -0.43 V re mg/HgO, 1 M kOh

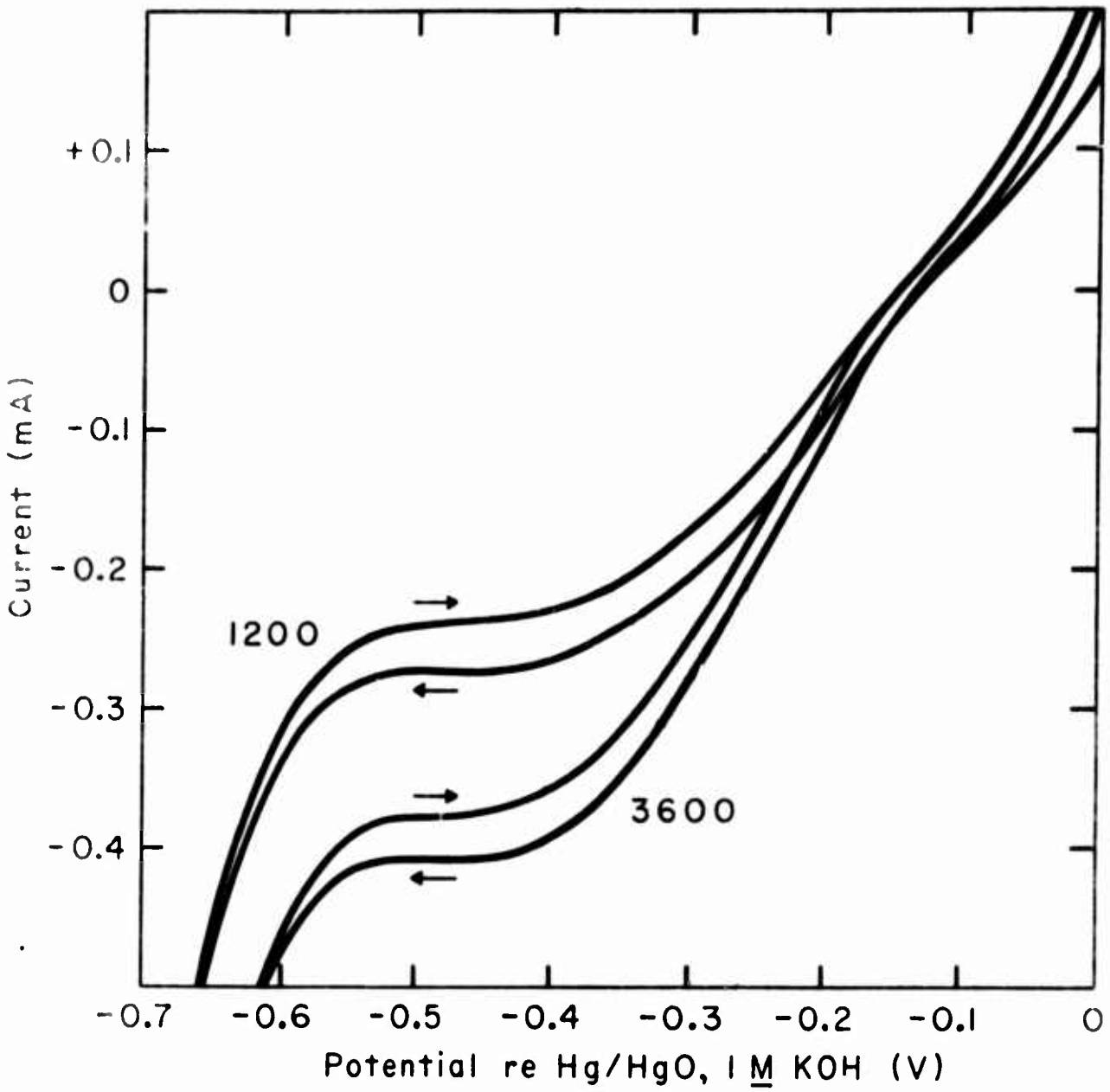

Figure 6. Reduction of O_2 on edge surface of high pressure annealed pyrolytic graphite with peroxide added. Electrolyte: 0.0047 M H_2O_2 + 0.953 M KOH, pressure O_2: 0.97 atm, temperature: 22°C, electrode area: 0.22 cm^2. Rotation rates indicated on curves in rpm.

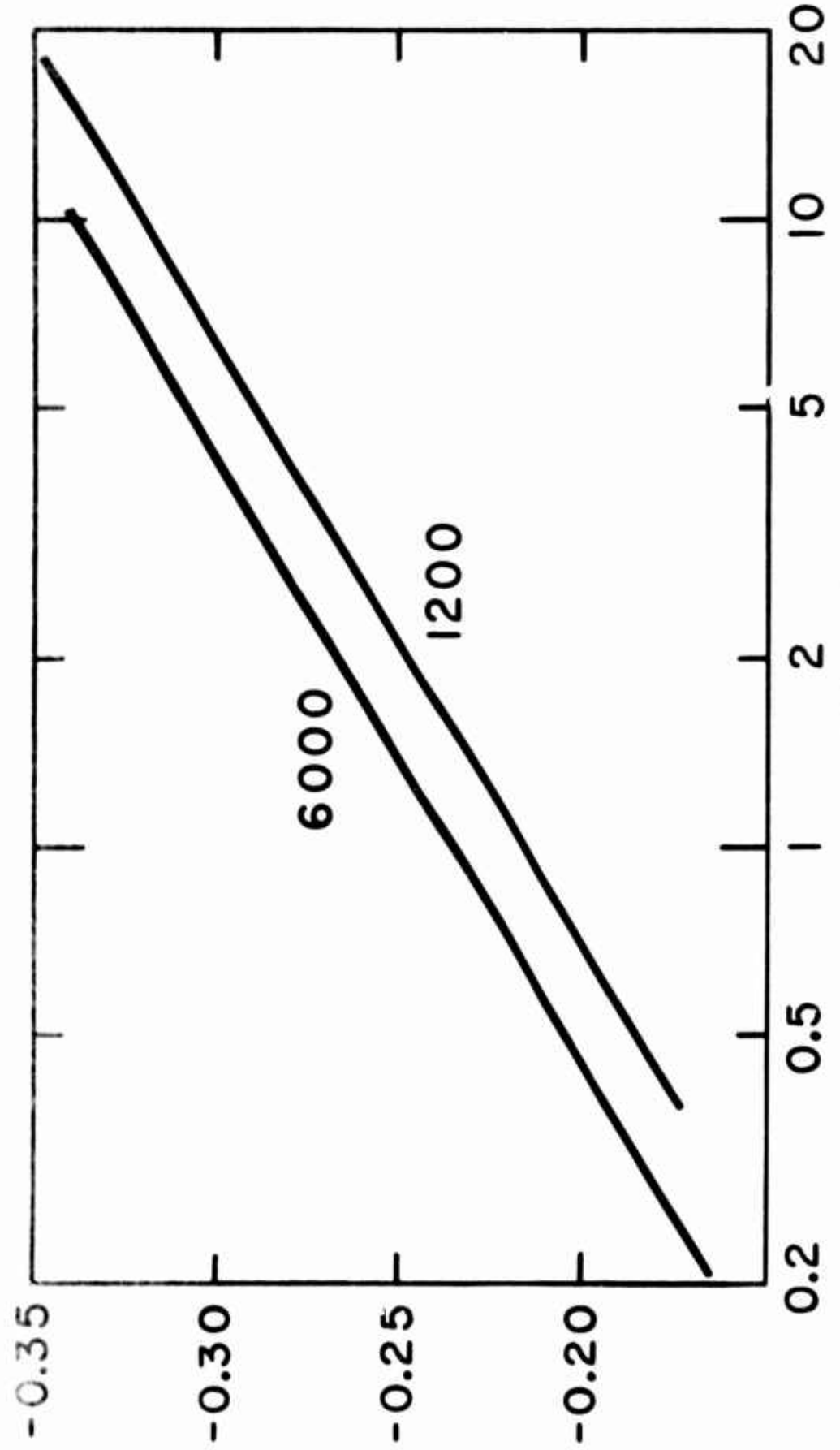

Figure 9. Reduction of O_2 on edge surface of high pressure annealed pyrolytic graphite. Conditions: same as for Fig. 2. Rotation rates indicated on curves in rpm. [Curves extend only over region where they could be established with reasonable accuracy from Fig. 2.]

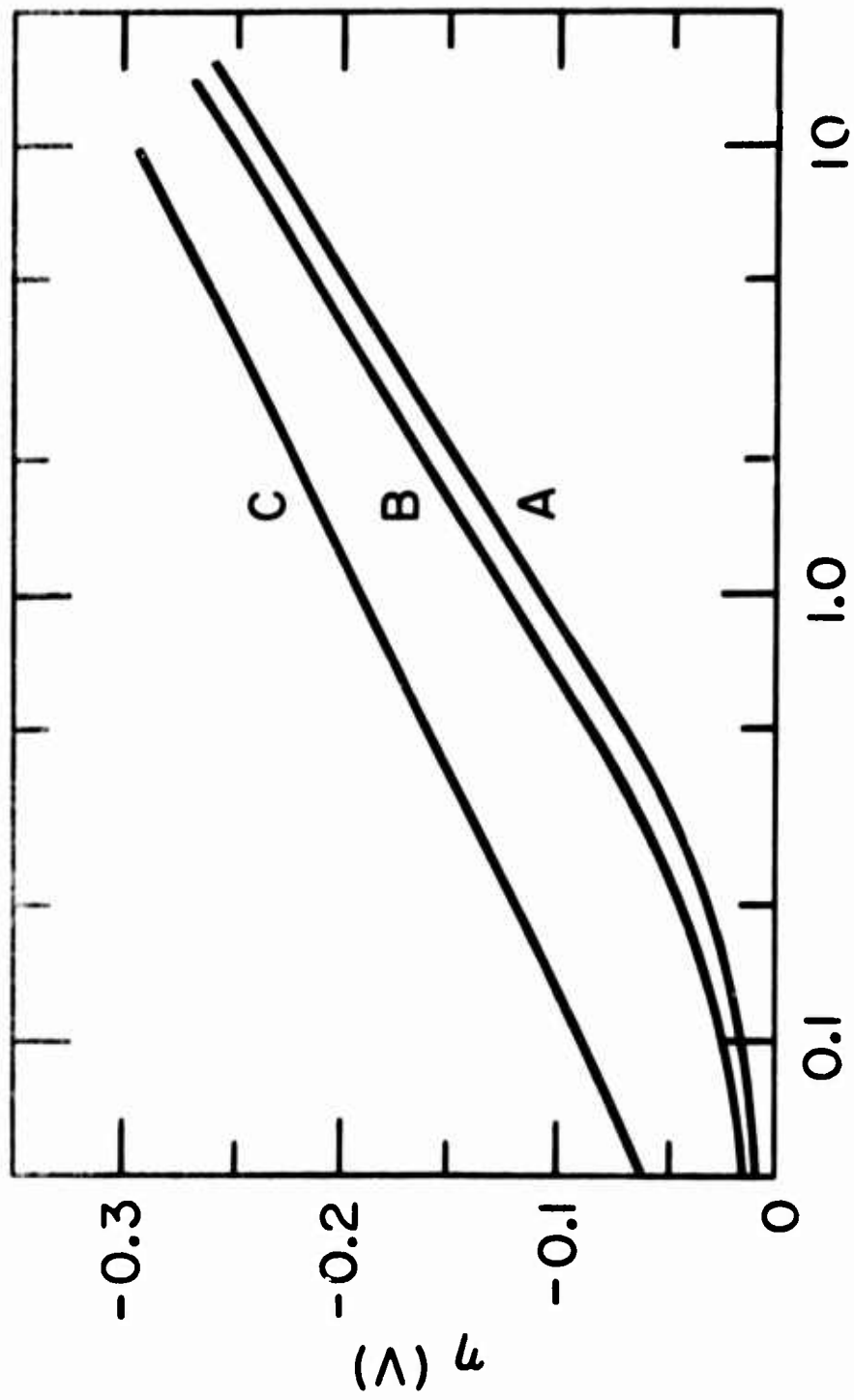

Figure 10. Overpotential plot for the reduction of O_2 on high pressure annealed pyrolytic graphite. Curve A - 1200 rpm, data from Fig. 8. Curve B - 3600 rpm, data from Fig. 8. Curve C - 4800 rpm, data from Fig. 11.

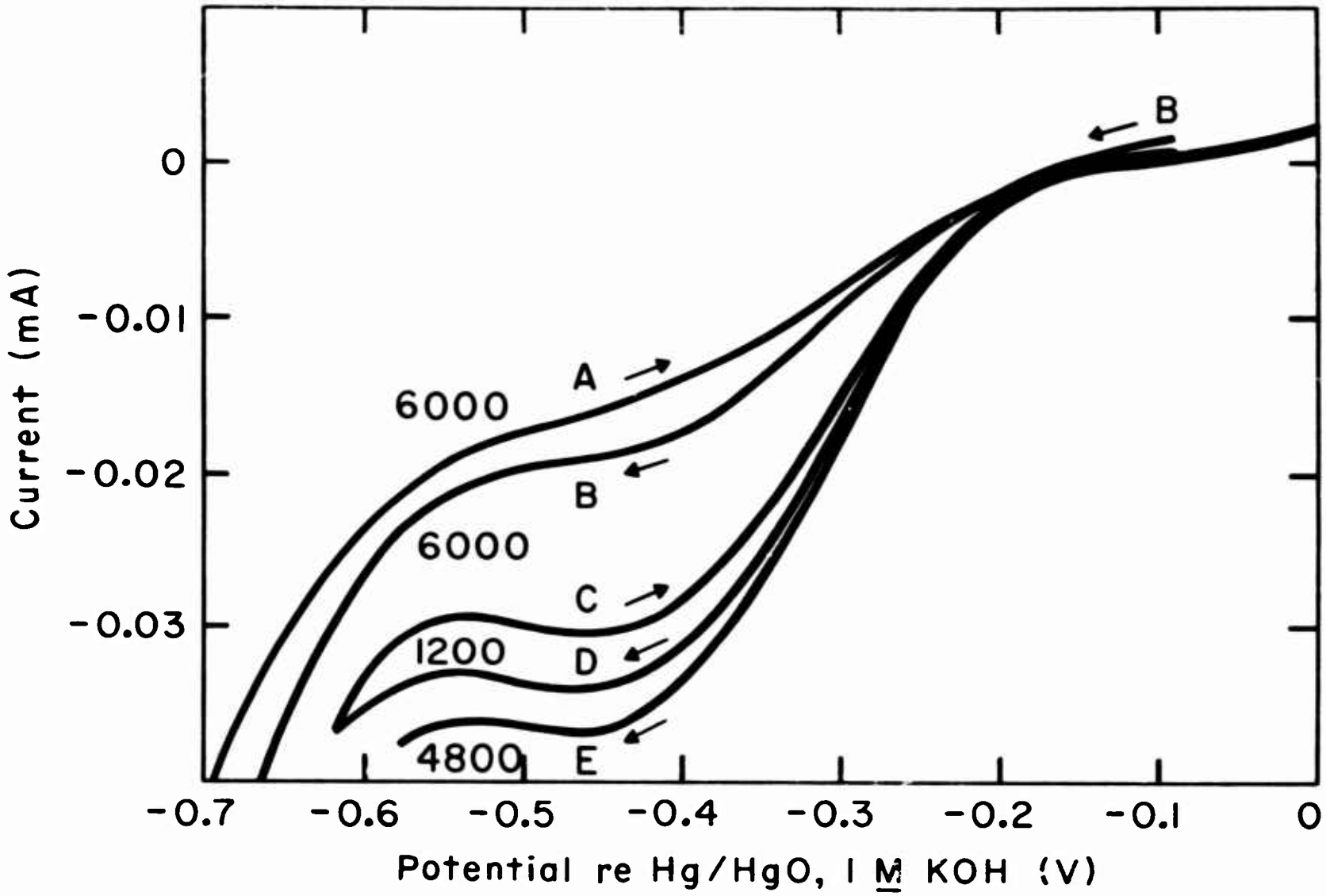

Figure 11. Reduction of O_2 on graphite. Pressure O_2: 0.97 atm, temperature: 22°C. Curves A,B: single crystal graphite, cleavage surface, area: 0.22 cm^2, electrolyte: 1 M KOH, rotation rate: 6000 rpm. Curves C,D,E: high pressure annealed pyrolytic graphite, cleavage surface, area: 0.196 cm^2, electrolyte: 0.07 M HO_2^- + 0.93 M KOH.

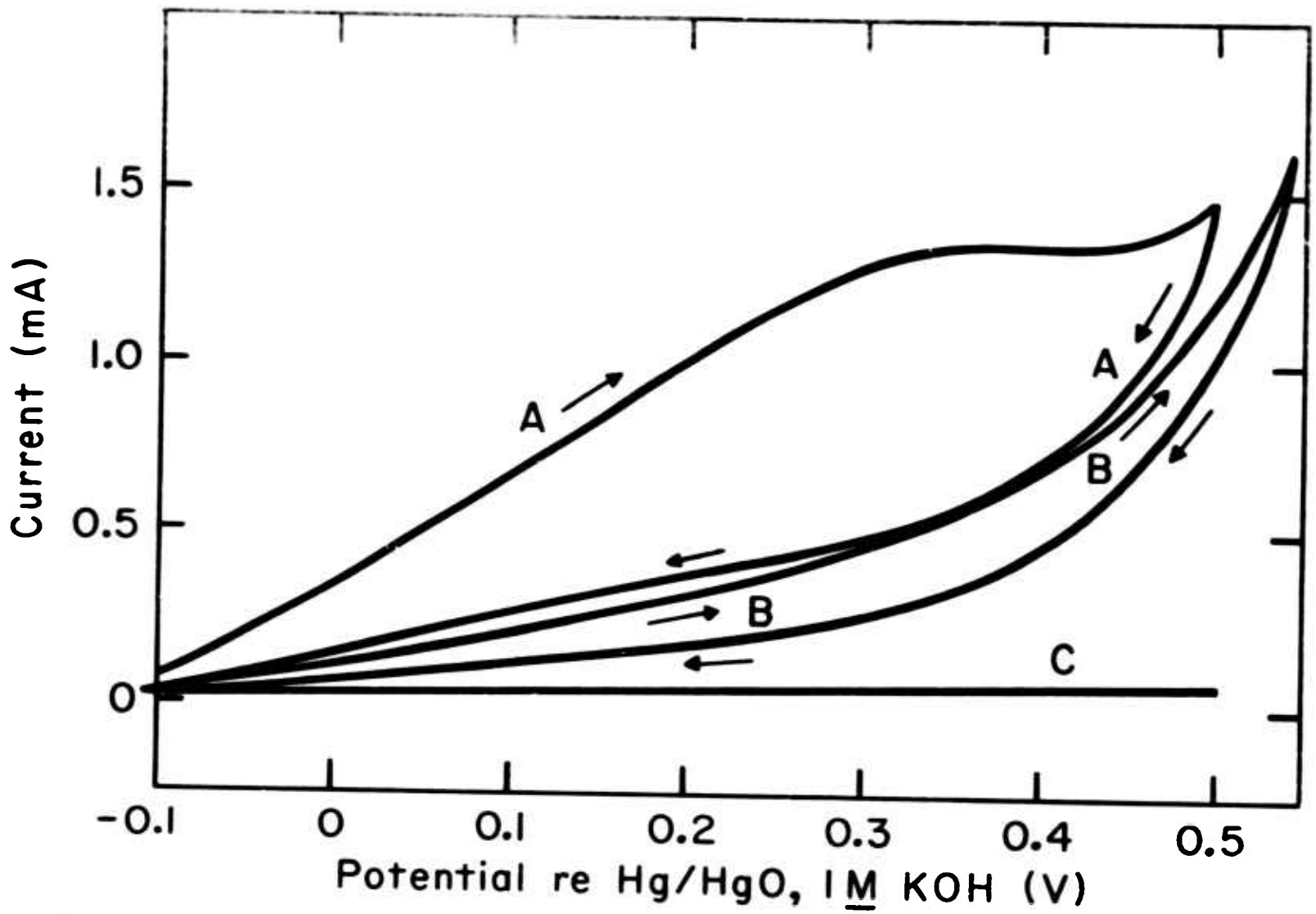

Figure 12. Oxidation of HO_2^- on high pressure annealed pyrolytic graphite. Electrolyte: 0.070 M HO_2^- + 0.93 M KOH, pressure O_2: 0.97 atm, temperature: 22°C, electrode area: 0.22 cm^2, rotation rate: 1200 rpm. Curve A: edge surface, 1st scan, Curve B: edge surface, 4th scan, Curve C: cleavage surface, 1st scan (either direction).

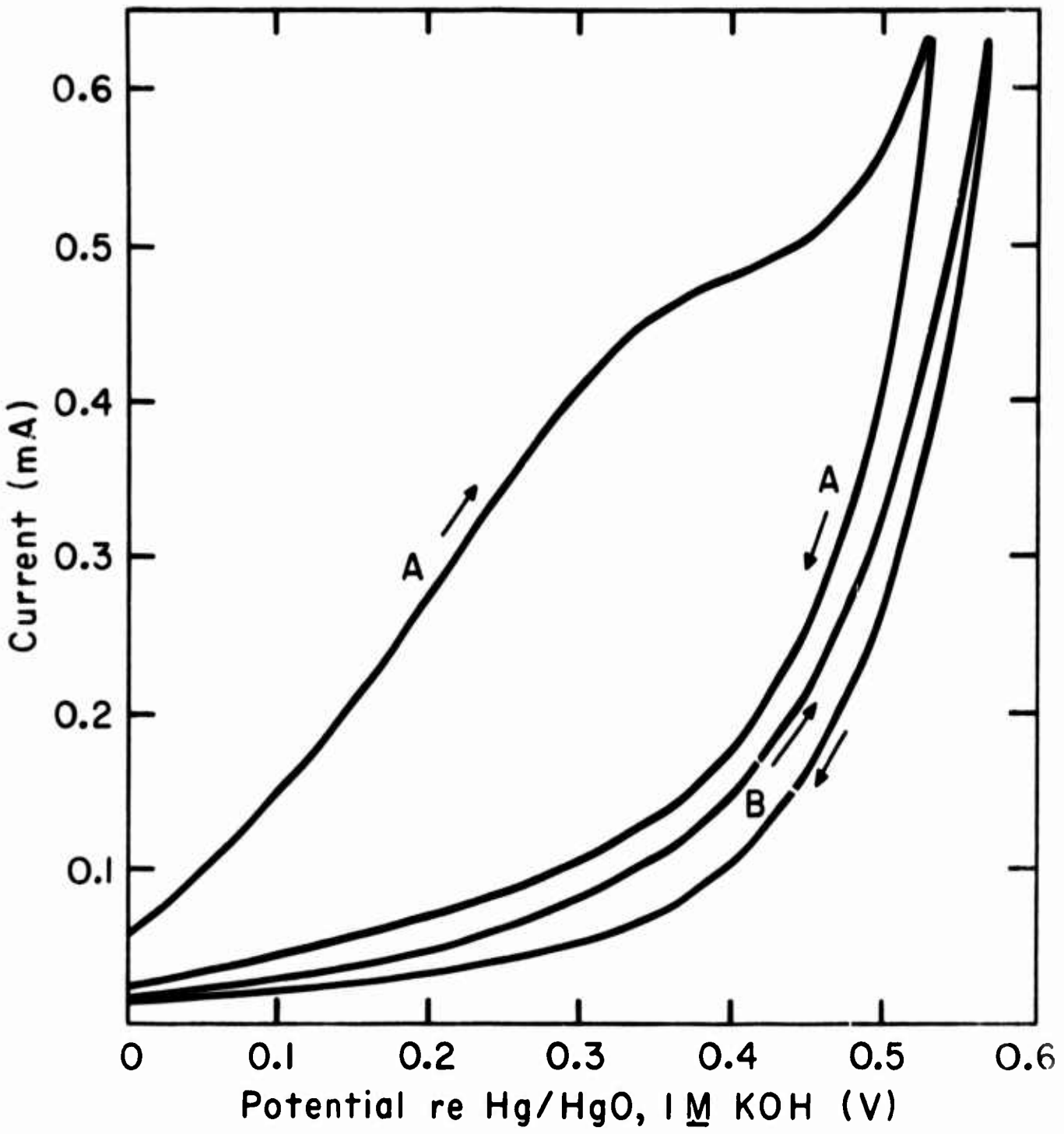

Figure 13. Oxidation of peroxide on cleavage surface of ordinary pyrolytic graphite. Electrolyte: 0.079 M HO_2^- + 0.921 M KOH, pressure O_2: 0.97 atm, temperature: 22°C, electrode area: 0.196 cm^2, rotation rate: 1200 rpm. Curves A: 1st scan, Curves B: 4th scan.

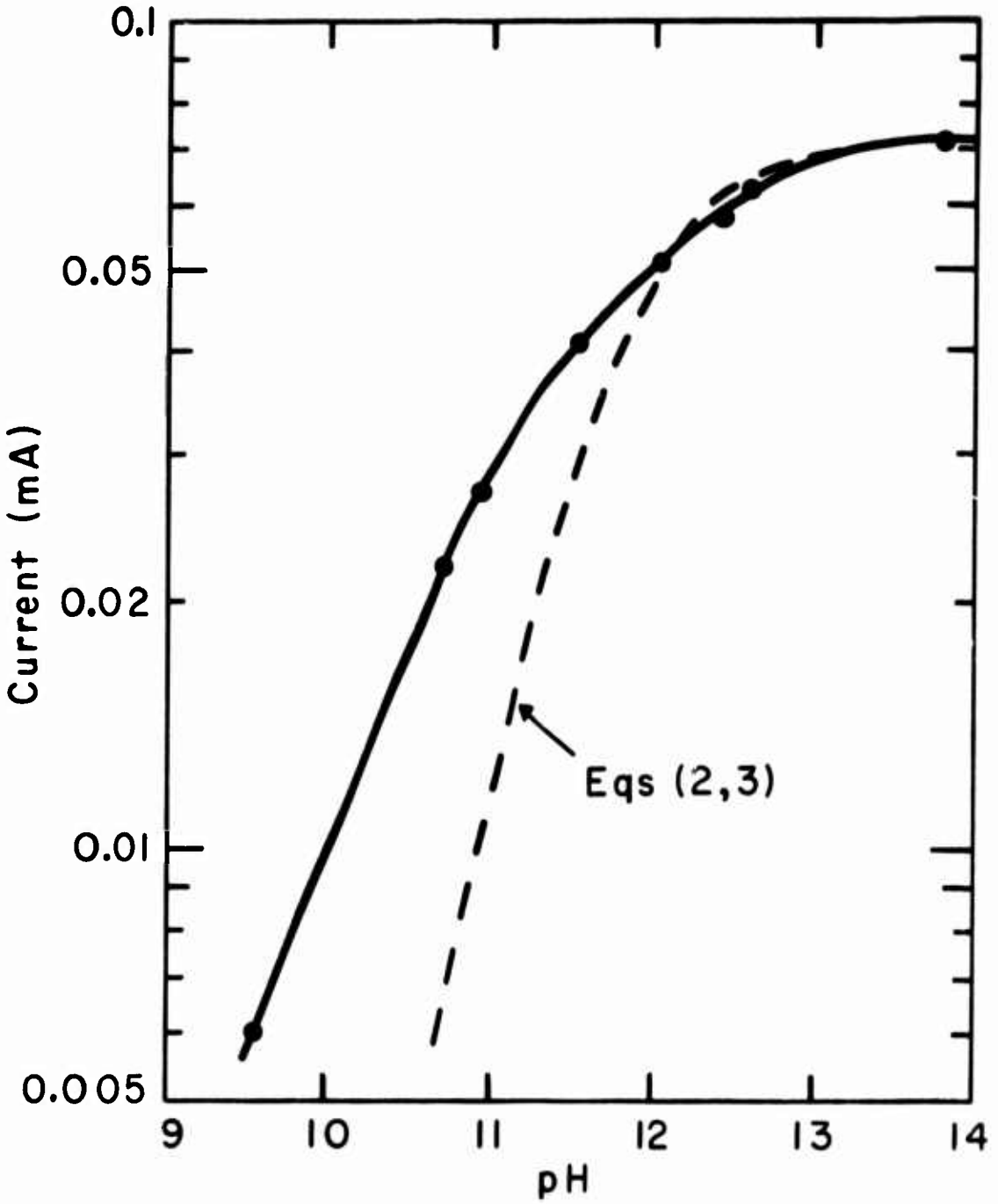

Figure 14. Dependence of oxidation of HO_2^- on pH for cleavage surface of ordinary pyrolytic graphite at constant electrode potential. Electrolyte: 1 M KOH + 0.078 M H_2O_2 + varying amounts of H_2SO_4, pressure O_2: 0.97 atm, temperature: 22°C, rotation rate: 1200 rpm, area: 0.196 cm^2, potential: 0.30 V re Hg/HgO, 1 M KOH.

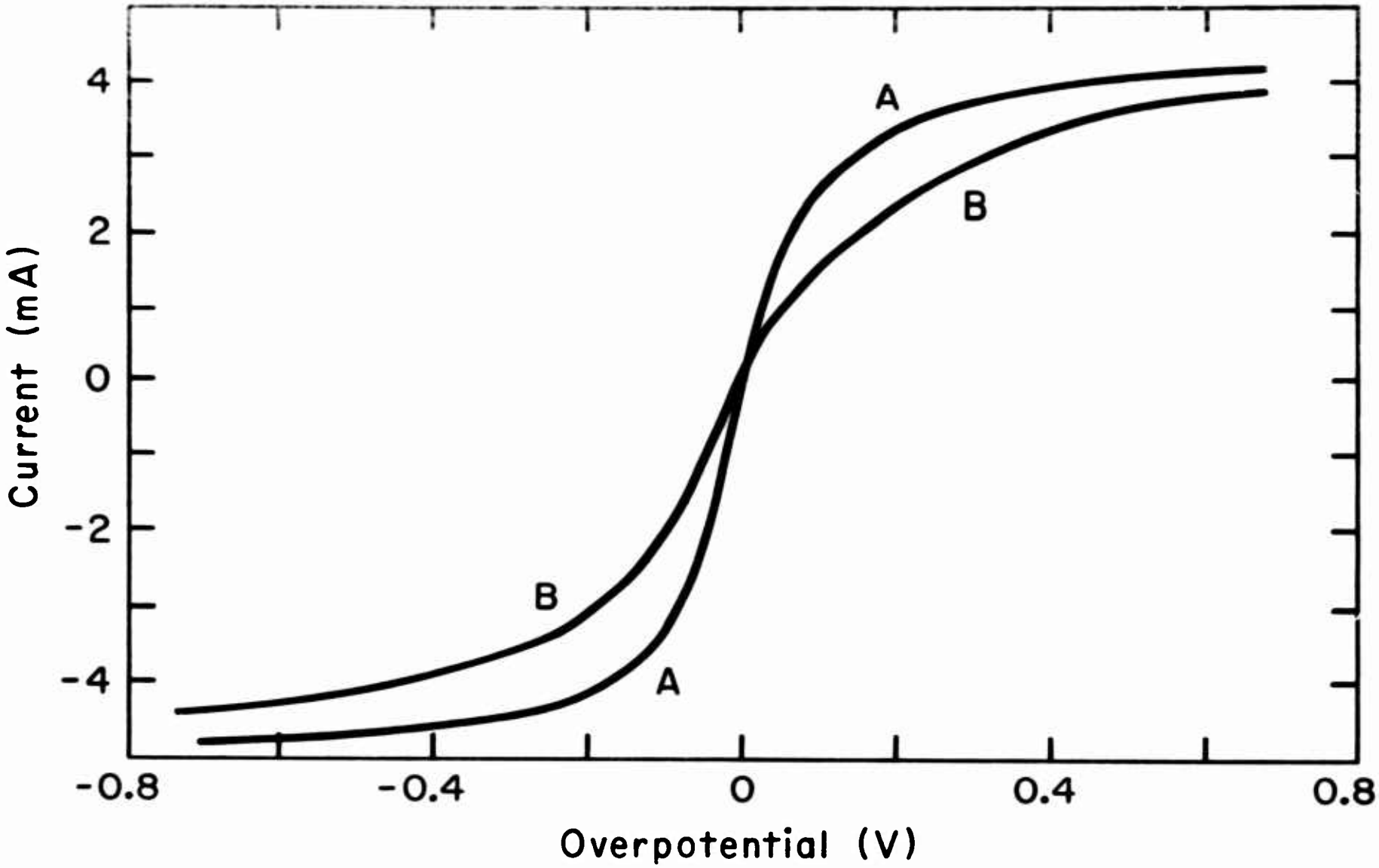

Figure 15. Overpotential curves for the ferri-ferrocyanide couple on high pressure annealed pyrolytic graphite. Electrolyte: 0.005 M $K_3Fe(CN)_6$ + 0.005 M $K_4Fe(CN)_6$ + 0.5 M K_2SO_4 adjusted to pH 3, temperature: 26°C, rotation rate: 3920 rpm. Curve A: edge surface. Curve B: cleavage surface.